



Comparison of physicochemical and thermal properties of choline chloride and betaine-based deep eutectic solvents: The influence of hydrogen bond acceptor and hydrogen bond donor nature and their molar ratios



Angelica Mero^a, Spyridon Koutsoumpos^b, Panagiotis Giannios^b, Ilias Stavarakas^b, Konstantinos Moutzouris^b, Andrea Mezzetta^a, Lorenzo Guazzelli^{a,*}

^a Università di Pisa, Dipartimento di Farmacia, via Bonanno 6, 56126 Pisa, Italy

^b Laboratory of Electronic Devices and Materials, Department of Electrical and Electronic Engineering, University of West Attica, Egaleo 12244, Greece

ARTICLE INFO

Article history:

Received 23 December 2022

Revised 15 February 2023

Accepted 28 February 2023

Available online 4 March 2023

Keywords:

Deep eutectic solvents

Rheological properties

Optical properties

Thermal properties

Effect of molar ratio

ABSTRACT

Within the green chemistry area, deep eutectic solvents (DESs) are playing an increasingly prominent role thanks to their intriguing physicochemical properties. However, a comparative study encompassing a wide range of properties as a function of different parameters such as the nature of the hydrogen bond acceptor (HBA) and donor (HBD) and their molar ratio is still missing. In this work, six DESs based on the most used HBAs (choline chloride (ChCl) and betaine (Bet)) and HBDs (ethylene glycol (EG), glycerol (Gly) and levulinic acid (LevA)) combined in three different molar ratio (1:2, 1:3, 1:4) have been prepared and subjected to a series of analysis aimed at measuring different properties such as density, viscosity, refractive index, thermal stability and thermal behaviour. The most striking findings see the EG-based DESs displaying the lowest density and viscosity values, while the Gly-based DESs exhibited the highest. High viscosity and density have been obtained using Bet instead of ChCl as HBA. Increasing the amount of HBD in DESs caused lower viscosity in all cases, while density increased for all Gly-based DESs and decreased for EG and LevA-based DESs. The refractive index also decreased when the HBD portion was increased. However, higher refractive index was obtained using ChCl instead of Bet as HBA. The temperature and wavelength dependence of the refractive index is otherwise described pretty well by a Sellmeier model. The molar refractivity implied by density and refractive index data via the Clausius-Mossotti equation is consistent with that predicted by the empirical but well-established model of Wildman and Crippen.

The short thermal stability of all investigated DESs is strictly related to the HBD used. EG-based DESs were less stable than LevA-based ones while Gly-based DESs were the most stable materials. Moreover, for all DESs three characteristic mass loss events have been identified. They can be attributed to the evaporation/degradation of the HBD, of the intimately interacting HBD-HBA and of the HBA, respectively. Finally, DSC analyses showed that all DESs can be used as solvents given that they are liquids at room temperature, and they maintain a liquid state in a broad range of temperatures ($T_g < -50$ °C or no thermal events are observed).

© 2023 The Authors. Published by Elsevier B.V. This is an open access article under the CC BY license (<http://creativecommons.org/licenses/by/4.0/>).

1. Introduction

The transition towards a sustainable growth requires great and radical changes in modern chemistry both in academia and in the industrial sector. In this context, the development of the green chemistry concept has prompted the scientific community to re-

sign processes by focusing on sustainability. The replacement of conventional organic solvents with the so-called green solvents is one of the main goals of the ecological transition. Indeed, classic organic solvents raise several concerns due to their toxicity and their high volatility and flammability. To overcome these issues, since their discovery by Abbott's team in the early 2000s [1], deep eutectic solvents (DESs) have attracted increasing attention and have been extensively investigated. DESs are defined as homogeneous eutectic mixtures obtained by mixing two or more pure

* Corresponding author.

E-mail address: lorenzo.guazzelli@unipi.it (L. Guazzelli).

components (liquids or solids, ions or neutral molecules) acting as hydrogen bond acceptor (HBA) and hydrogen bond donor (HBD). The “deep” nature is related to the significant negative temperature divergence observed at the eutectic point from the predicted temperature of the ideal liquid mixture [2]. DESs show a great number of interesting features [3] such as relative low volatility and flammability as well as a very simple preparation that does not require the use of solvents. The use of natural compounds or compounds derived from natural sources makes possible to obtain DESs with a particularly low environmental impact (natural DESs or NADESs) [4]. Similarly to ionic liquids, the main attractive feature of DESs is the tunability of their physicochemical properties that allows for defining them as designer solvents. Indeed, the possibility to pair a large number of diverse HBA and HBD in different molar ratios allows in theory the preparation of DESs with specific properties in terms of density, viscosity, polarity, refractive index, ionic conductivity, surface tension, thermal and chemical stability and phase behavior [3–6].

DESs have been used in a broad range of research areas, for instance as media or catalyst for organic synthesis [7,8], enantiodiscrimination media in electroanalysis [9], as extraction solvents for bioactive molecules [6,10–12] such as polyphenols [13–15] or for removing metal ions or other contaminants from water and different media [7,16], as well as medium for terrestrial and marine [17] biomass treatment [3,18–21]. Furthermore, DESs have been employed in the pharmaceutical field [3] as drug delivery media or solubilizing systems [6,22] or therapeutic systems [23], in material chemistry [3,24], as media for CO₂ and SO₂ absorption [3,25] or in enzymatic biotransformation processes [26] and in electrochemistry [27].

The first HBA reported was choline chloride (ChCl), also known as vitamin B₄, due to its numerous advantageous features. Indeed, ChCl is cheap, readily available, highly biodegradable, non-toxic and is approved as a feed additive for several animal species [28,29]. Although numerous quaternary ammonium salts and other compounds have been used as HBA, ChCl is still the most commonly used thanks to its strong propensity to form intermolecular interactions [30]. More recently, the zwitterionic trimethylglycine, commonly called betaine (Bet), has gained increasing interest as an alternative to ChCl as HBA in the pursuit towards the synthesis of novel DESs. Bet presents the same positively charged ammonium moiety of ChCl and a carboxylate group and the resulting inner salt nature confers it a number of distinctive features. Furthermore, Bet is a non-toxic, readily biodegradable osmolyte playing fundamental roles in cells of most living organisms. In contrast to the ChCl available on the market, which is a synthetic product, Bet derives from renewable sources since it is a by-product of sugar production [30]. For what concerns natural-derived HBD partners, the most employed classes are polyols, such as ethylene glycol (EG) and glycerol (Gly), sugars and carboxylic acids. Among this latter class of HBDs, levulinic acid (LevA) shows appealing properties as it can be readily obtained from cellulose and is widely available at low cost [31–33]. ChCl and Bet based-DESs with EG, Gly and LevA as HBDs have been largely studied and found applications in several fields. To date, numerous publications reported the measurement of some of the physicochemical properties of these DESs, especially of ChCl-based ones, and more specifically of ethaline (ChCl:EG 1:2) [34–37] and glyceline (ChCl:Gly 1:2) [38–40]. However, these studies only focussed on the characterization and the comparison of these DESs. Indeed, in most cases specific properties have been investigated in order to evaluate the suitability of these DESs for an application of interest [41–45]. In this context, a comprehensive study describing the properties of the DESs is still lacking despite its potential general interest. Needless to say, the understanding of the influence of HBA, HBD and their molar ratio on the DESs behaviour will make

for a better partner selection given a target application and for a conscious design of large-scale processes [46]. Moreover, the collection of a robust data set as a function of different parameters is key to the development of a reliable theoretical model for the prediction of the properties of new DESs. In this work, different families of DESs based on ChCl or Bet as HBAs, and EG, Gly and LevA as HBDs, were prepared at three molar ratios (1:2; 1:3; 1:4) and their physicochemical and thermal properties were measured and compared. Density, viscosity and optical properties were first evaluated as a function of the temperature. Afterwards the thermal properties were determined to assess their thermal stability and behaviour.

2. Materials and methods

Choline chloride 98 % (ChCl), betaine anhydrous > 97 % (Bet), ethylene glycol 99 % (EG) and levulinic acid 98 % (LevA) were purchased by Alfa Aesar, Thermo Fisher. Glycerol (Gly) 99 % was purchased from Sigma-Aldrich (Merck Life Science).

2.1. DES preparation

Prior to the DES preparation, ChCl, EG, Gly and LevA were accurately dried under vacuum for 6 h at 80 °C. Briefly, ChCl or Bet and the corresponding HBD (EG, Gly and LevA) were mixed in different molar ratios at room temperature until a homogenous transparent liquid was formed; see Table 1. After DES formation, no purification step was needed. The DESs were further dried under vacuum for 24 h at 60 °C to ensure the removal of water and they were kept at room temperature in sealed vessels until their use. The purity and the composition of DESs was ascertained by ¹H NMR analysis (D₂O), reported in Supplementary File (Figs. S1–S6).

2.2. NMR spectroscopy

¹H NMR spectra were recorded in D₂O, on a Bruker 400 MHz NMR spectrometer at 25 °C. ¹H NMR chemical shifts (ppm) are referenced to residual D₂O (δ_{H} 4.79). All samples were analyzed at fixed concentration (30 mg/cm³).

2.3. Water content determination

The water content of DESs was estimated by Karl Fischer titration using a SI Analytics coulometer (Titroline 75 000 KFtrace).

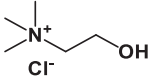
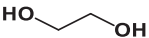
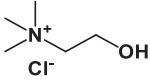
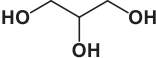
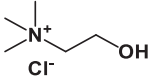
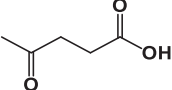
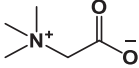
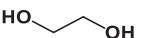
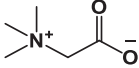
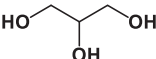
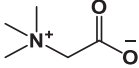
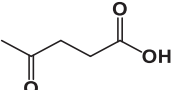
2.4. Density

Densities of DESs at different temperatures were measured using a density-meter (Anton Paar, DMA 4500 M). This instrument exploits a U-shaped oscillating tube as a sensing element. Measurements were collected in the temperature range from 20 to 90 °C. Densimeter calibration was conducted by using the reference density values of water, which was obtained from the fundamental equation of state by Wagner and Pruss (uncertainty lower than ± 0.003 % in the full pressure and temperature ranges).

2.5. Viscosity

Viscosities of DESs as a function of temperature were measured using a modular compact rheometer (MCR 302, Anton Paar) equipped with a plate-plate geometry (diameter of 5 cm) and a protective hood. Before conducting the measurements, the samples were subjected to a pre-shear to get uniform and homogeneous samples on the plate. First of all, flow curve measurements were carried out by varying the shear rate from 100 to 1000 s⁻¹ at

Table 1
DESs studied in this work.

| Name | HBA | HBD | Molar ratio | Physical Appearance |
|-----------|---|---|-------------|---|
| ChCl:EG |  |  | 1:2 | Transparent liquid |
| | | | 1:3 | Transparent liquid |
| | | | 1:4 | Transparent liquid |
| ChCl:Gly |  |  | 1:2 | Transparent liquid |
| | | | 1:3 | Transparent liquid |
| | | | 1:4 | Transparent liquid |
| ChCl:LevA |  |  | 1:2 | Transparent liquid |
| | | | 1:3 | Transparent liquid |
| | | | 1:4 | Transparent liquid |
| Bet:EG |  |  | 1:2 | Transparent liquid with white precipitate |
| | | | 1:3 | Transparent liquid |
| | | | 1:4 | Transparent liquid |
| Bet:Gly |  |  | 1:2 | Transparent liquid |
| | | | 1:3 | Transparent liquid |
| | | | 1:4 | Transparent liquid |
| Bet:LevA |  |  | 1:2 | Transparent liquid |
| | | | 1:3 | Transparent liquid |
| | | | 1:4 | Transparent liquid |

20 °C. 37 data points were collected by the rheometer every 15 s. Then, the effect of increasing temperature was tested, performing the measurements in the temperature range from 20 to 90 °C applying a constant shear rate at which all mixtures behave as Newtonian liquids. The temperature of the instrument was controlled by a Water-Cooled Peltier system (H-PTD200, Anton Paar).

2.6. Thermal gravimetric analysis (TGA)

The thermal stability of DESs and their components was investigated by thermal gravimetric analysis (TG) conducted in a TA Instruments Q500 TGA (weighing Precision \pm 0.01 %, sensitivity 0.1 μ g, baseline dynamic drift < 50 μ g). The temperature calibration was performed using Curie point of nickel and Alumel standards and for mass calibration weight standards of 1 g, 500 mg, and 100 mg were used. All the standards were supplied by TA Instruments Inc. 12–15 mg of each sample were heated in a platinum crucible as sample holder. First, the heating mode was set to isothermal at 60 °C in N₂ (80 cm³/min) for 30 min. Then, the sample was heated from 40 °C to 500 °C at 10 °C/min under nitrogen (80 cm³/min) and maintained at 500 °C for 3 min. Mass change was recorded as a function of temperature and time. TGA experiments were carried out in triplicate.

2.7. Differential scanning calorimetry (DSC)

The thermal behavior of DESs was analyzed by a differential scanning calorimeter (TA DSC, Q250, USA, temperature accuracy \pm 0.05 °C, temperature precision \pm 0.008 °C, enthalpy precision \pm 0.08 %). Dry high purity N₂ gas with a flow rate of 50 cm³/min was purged through the sample. 1–5 mg of each sample was loaded in pinhole hermetic aluminium crucibles and the phase behavior was explored under nitrogen atmosphere in the temperature range from –90 to 100 °C with a heating rate of 10 °C/min. The temperature calibration was performed considering the heating rate dependence of the onset temperature of the melting peak of indium. The enthalpy was also calibrated using indium (melting enthalpy $\Delta H_m = 28.71$ J/g). DSC experiments were carried out in duplicate. T_g was obtained by taking the midpoint of the heat capacity change on heating from a glass to a liquid. T_m and T_{cc} were taken as the peak temperature of the endothermic peak on the

heating run while T_c as the peak temperature of the exothermic peak on the cooling run.

2.8. Refractive index

The refractive index was measured for five wavelengths (450 nm, 532 nm, 633 nm, 964 nm, 1551 nm) each for temperatures from 30 °C to 100 °C with the same Metricon 2010/M refractometer previously utilized by the authors[47] and described in more detail elsewhere[48,49]. Before commencing with the main measurement, each sample was preheated at 100 °C and the refractive index at 633 nm was measured every 10 min for at least an hour in a preliminary stability and reproducibility check. After stability and reproducibility was ensured, a temperature controller let the sample cool down in steps of 5 °C and the refractometer automatically determined the refractive index by the acquired reflectance profile around the angle of total internal reflection for each of the five available wavelengths at the resulting stabilized (within \pm 0.5 °C) temperature. The refractometer's angular resolution of 0.004° leads to an uncertainty of \pm 0.0002 in the determined refractive index. Since cooling slows down appreciably close to ambient temperature, temperature steps were often increased to 10 °C or even 20 °C below 50 °C, for a last measurement at 30 °C. In each case, we checked for water absorption from the exposed surface of the DES, which was not an issue for the duration of the measurement except for ChCl:Gly 1:4. It should be noted that prolonged overnight exposure of the measured samples to the air at ambient temperature always led to a substantial decrease of the refractive index, which could be slowly reversed by reheating the sample, indicating water absorption.

3. Results and discussions

3.1. DES preparation

All eutectic mixtures were prepared through simple mixing of the selected HBA and HBD at room temperature until the obtainment of homogeneous liquids (please refer to Table 1, Section 2.1). Considering the influence that the water content has on the final mixtures' properties, prior to the synthesis, ChCl, EG, Gly and LevA were accurately dried under vacuum. Instead, betaine was purchased in anhydrous form and did not require further drying. Fur-

thermore, after preparation the obtained DESs were further dried under vacuum and their water content was determined by Karl Fisher titration before all measurements. The water content was below 400 ppm for DESs containing LevA and in the range 400–600 ppm for DESs containing EG and Gly. The purity and the right molar ratio of prepared DESs was ascertained by ^1H NMR analysis (Figs. S1–S6). Bet:EG 1:2 was obtained as a transparent liquid with a white precipitate, even after stirring and heating the mixture up to 80 °C. For this reason, this system was excluded from the following study.

3.2. Density

Density data for some of the DESs studied in this work, especially ChCl based-DESs with EG and Gly, have been reported for specific temperatures [50,51] or as a function of temperature. In particular, systematic investigations of density dependence on temperature and the one or the other molar ratio for these compounds have been performed by different groups [34,36–40,52–56]. Similar investigations have been carried out for ChCl DESs with LevA [44,57–59] and Bet DESs with LevA [42,43,60,61]. To the best of our knowledge, data for the temperature dependence of density for Bet DESs with EG and Gly have been reported only for the 1:3 molar ratio [41,62,63] and also for Bet:Gly 1:2 [63,64].

Despite the large number of relevant publications, the reported density data are still incomplete, in the sense that some DES families (e.g. ChCl:EG and ChCl:Gly) and molar ratios (eg 1:2) are over-represented while others are underrepresented or even missing. A comprehensive and representative database of physical properties of DESs is fundamental in the construction of empirical predictive models for hitherto unstudied DES families. Density is especially important because it relates to other physical and optical properties by established physical laws (please refer to Section 3.5).

The density of all DESs studied in this work was measured with a step of 5 °C for temperatures between 20 °C and 90 °C and the obtained values are reported in Tables S1–S3. In all cases density was higher than water and decreased linearly by increasing temperature, as demonstrated by the plots of Fig. 1. Linear regression describes the temperature dependence always with $R^2 > 0.9999$ in the measured range. The resulting optimal slopes and intercepts of the linear model are tabulated in Table 2 for each DES and molar ratio. The densities of the pure HBDs were also measured and compared to the prepared DESs. An influence of both the HBA and HBD was detected. Indeed, all Bet-based DESs displayed higher densities than their counterparts containing ChCl as HBA. Instead, regarding the HBD, the density decreased in the following order Gly > LevA > EG within the same families of DESs. Unsurprisingly, considering the high density of pure Gly (from 1.25956 g/cm³ at 20 °C to 1.21376 g/cm³ at 90 °C), Gly-containing DESs were the systems with the highest densities, which increased as a function of the Gly amount. Among the Gly-containing solvents, Bet:Gly 1:4 showed the highest density. Specularly, giving the density value of pure EG (from 1.11147 g/cm³ at 20 °C to 1.06058 g/cm³ at 90 °C), EG-containing DESs were the less dense solvents. LevA-containing DESs showed an intermediate behaviour characterized by higher densities than pure LevA. Interestingly, no significant differences were noticeable for the three molar ratios in the case of ChCl-based DESs. As previously reported in the literature, the higher the number of —OH functional groups in the HBD (Gly vs EG), and thus the increased possibility of hydrogen bonds' formation, the higher the density of the system [6]. This trend has been widely reported by Basaiahgari et al. who found lower densities for DESs composed of benzyl trialkylammonium chloride salts as HBAs and EG as HBD than DESs with the same HBA and either diethylene glycol, triethylene glycol, or Gly as HBDs [65]. In the same way, carbohydrates-based DESs exhibited higher values of density

[66]. Intermolecular interactions, hence, represent one of the main factors influencing density. In the cases studies here, also the different nature of the HBA plays an active role considering that ChCl principally participates in the hydrogen bonding network through the chloride anion [67] while Bet via the carboxylate group.

Based on the hole theory, it has also been speculated that the density of a DES, as well as other properties, is strictly related to the size and shape of the mixture's components as well as the available free space in the structure of the mixture. Indeed, the molecular structure of a DES can contain empty vacancies or holes, the size of which will determine the systems' density [63]. This could further explain the different behaviour of Bet and ChCl-based DESs: the small zwitterionic betaine can lead to more compact systems than the salt ChCl. The influence of the HBA can be further confirmed by analyzing the density data reported for *N,N*-diethanolammonium chloride:EG or Gly DESs [68]. Indeed, although the HBA differs from ChCl for only one methyl group, lower values of densities were obtained. Also, for tetrabutylammonium chloride:EG 1:2 much lower values of density have been reported due to the higher steric hindrance of the HBA when compared to ChCl, that led to a worse packing of molecules. It is worth mentioning that the HBA and HBD molar ratio can be used to manipulate the density of a DES. Also, the higher number of hydrogen bonds reduces the free spaces available and consequently increases the density of DESs [69,70]. All these considerations are in agreement with the highest density registered for Bet:Gly 1:4.

Additionally, the free space in the DES may increase at higher temperatures due to the reduction of the number of hydrogen bonds, leading to a faster movement of molecules, and a reduction in density of the DES [68].

A physical property with considerable explanatory power, which is readily determined by the temperature dependence of density, is the volumetric thermal expansion coefficient β defined by

$$\beta = \frac{1}{V} \left(\frac{\partial V}{\partial T} \right)_p = -\frac{1}{\rho} \left(\frac{\partial \rho}{\partial T} \right)_p \quad (1)$$

The coefficient of thermal expansion is a measure of the ease with which a liquid expands when heated under constant pressure. Since our observations revealed a linear density dependence on temperature for the investigated DESs, thermal expansion coefficient is simply calculated by the formula $\beta = (B/|A| - T)^{-1}$, where A, B are the parameters of the linear model listed in Table 2.

Fig. 2 further suggests that the thermal expansion coefficient increases when the molar ratio of the specific HBD increases. It also increases in the order LevA > EG > Gly among the investigated HBDs and Bet > ChCl among HBAs. Considering that LevA, EG, and Gly can form at most 1, 2, and 3 hydrogen bonds respectively, it appears that the coefficient of thermal expansion increases when the possibility of hydrogen bond formation are reduced. By the same token, the possibilities of hydrogen bond formation appear to be lower for DES with betaine as a HBA instead of choline chloride.

Since hydrogen bonds tend on average to keep molecules closer together than they would otherwise be, it is reasonable to assume that a liquid with more hydrogen bonds would expand less easily when heated, resulting in a correspondingly lower coefficient of thermal expansion.

It is noteworthy to point out that the thermal expansion coefficients of the LevA-based DESs, especially at 1:4 molar ratio, are very close to the β values of the most commonly used commercial heat-transfer fluids (Therminol 66 and Marlotherm SH) in the same range of temperatures [71]. Conversely, EG and Gly-based DESs show slightly lower values and, among them, ChCl:Gly 1:2 and Bet:Gly 1:2 display the lowest values. The regular behavior of the

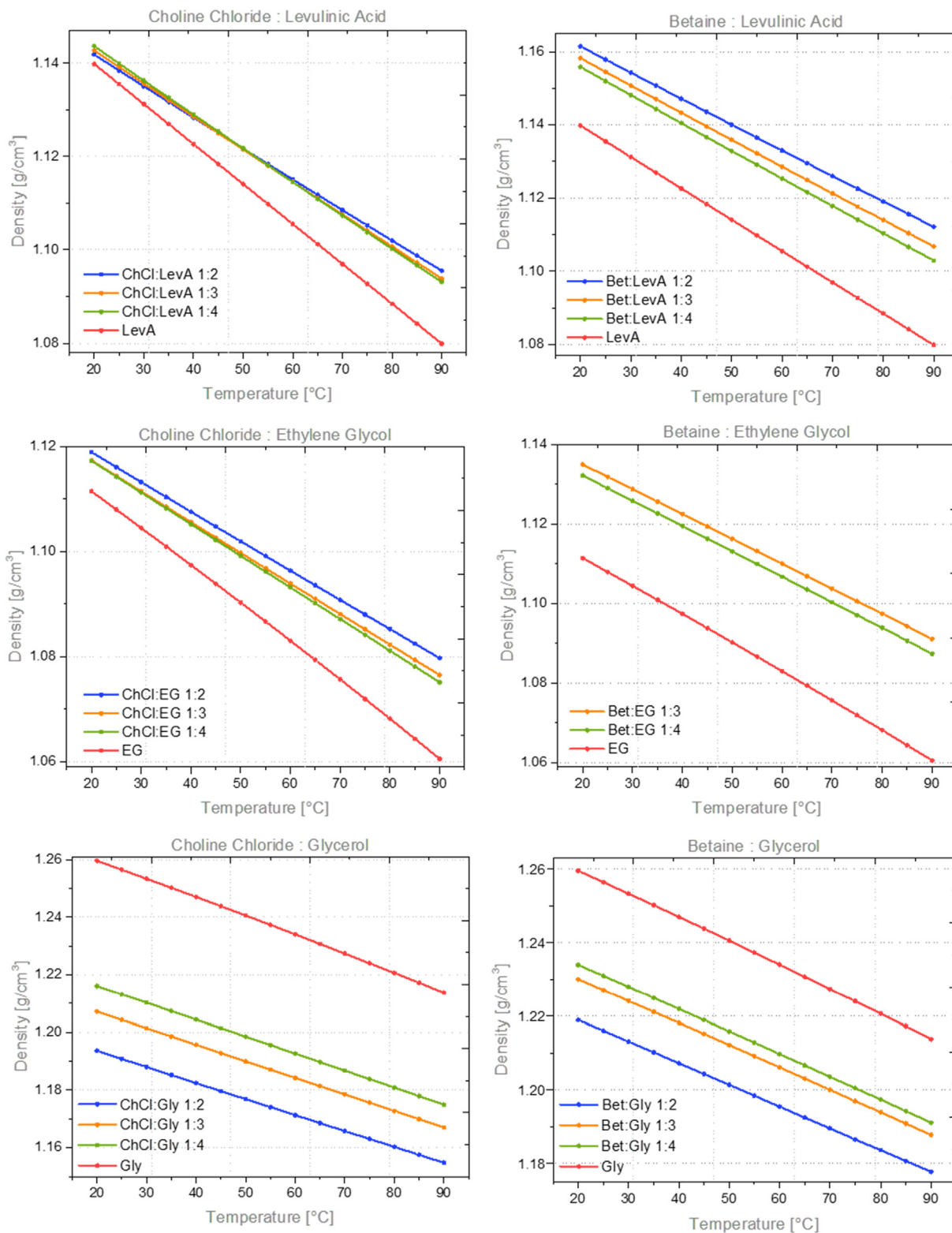


Fig. 1. Density dependence on temperature for the indicated DES and molar ratio. Dots are measurements while solid lines are linear model fits with the parameters of Table 2.

thermal expansion coefficient in Fig. 2 should be contrasted with the behavior of density in Fig. 1 where, except of course for the linear decrease, there is no other immediately obvious universal pattern that would lend itself to physical interpretation.

To conclude with all the properties related to density, molar volume (V_m) of DESs can be calculated from experimental density data by the following equation:

$$V_m = \frac{M_{DES}}{\rho} \tag{2}$$

Table 2

Optimal parameters of the linear model $\rho = AT + B$ for the temperature dependence of density from 20 °C to 90 °C, for the indicated DES and molar ratio.

| DES | Molar Ratio | $-10^4 A [^\circ\text{C}]^{-1}$ | $B [\text{g}/\text{cm}^3]$ |
|-----------|-------------|---------------------------------|----------------------------|
| ChCl:LevA | 1:2 | 6.61557 | 1.15486 |
| | 1:3 | 6.98443 | 1.15652 |
| | 1:4 | 7.21636 | 1.15788 |
| ChCl:EG | 1:2 | 5.59543 | 1.12999 |
| | 1:3 | 5.82886 | 1.12892 |
| | 1:4 | 6.01579 | 1.12927 |
| ChCl:Gly | 1:2 | 5.54789 | 1.20467 |
| | 1:3 | 5.72636 | 1.21862 |
| | 1:4 | 5.87493 | 1.22789 |
| Bet:LevA | 1:2 | 7.04986 | 1.17540 |
| | 1:3 | 7.35064 | 1.17277 |
| | 1:4 | 7.55557 | 1.17076 |
| Bet:EG | 1:3 | 6.26479 | 1.14760 |
| | 1:4 | 6.39300 | 1.14508 |
| | 1:2 | 5.89929 | 1.20378 |
| Bet:Gly | 1:3 | 6.04621 | 1.24229 |
| | 1:4 | 6.12679 | 1.24638 |

where M_{DES} and ρ are the molar mass and the density of DESs, respectively. The molar mass was calculated using the following equation:

$$M_{\text{DES}} = X_{\text{HBA}} * M_{\text{HBA}} + X_{\text{HBD}} * M_{\text{HBD}} \quad (3)$$

where X and M are the molar ratio and the molar mass of the HBA and HBD denoting as subscripts.

As observed from the data reported in Tables S4–S6 and depicted in Fig. 3, higher values were obtained increasing the molar ratio from 1:2 to 1:4 for all the investigated families of DESs. Moreover, as expected, the molar volumes increased with increasing molar mass of each compound. Indeed, higher values were detected for ChCl-based DESs while considering the same HBA (both Bet and ChCl) and molar ratio, the molar volume decreased in the following order: LevA > Gly > EG. Finally, the variation of V_m with temperature is similar for all DESs, that is V_m slightly increased when temperature increased [60,72].

3.3. Viscosity

The viscosity of DESs represents another fundamental parameter which contributes to transport properties and thus can be used to define their possible applicability as reaction or extraction media, especially from an industrial point of view.

As mentioned previously for density data, also viscosity values for some of the DESs investigated in this work, again especially those composed of ChCl and polyols, have been already reported by different groups. In particular, measurements at specific temperatures and in some cases as a function of temperature have been carried out, principally for so-called ethaline and glyceline (ChCl:EG 1:2 and ChCl:Gly 1:2) [38,51,73–75] and their mixtures with water, methanol or dimethyl sulfoxide [36,76,77]. For these systems, sporadically also the influence of the molar ratio on the viscosity has been evaluated (from 1:2 to 1:6 for ChCl:EG DESs [37,39,78] and from 1:2 to 1:5 for ChCl:Gly DESs [40,45,69]). Similar investigations were performed for ChCl:LevA DESs, particularly for 1:2 molar ratio [44,57,59]. Once again, for Bet based-DESs with EG, Gly and LevA as HBDs, only few works have been reported on their rheological properties [41,42,60,61,63,64], despite the increasing number of studies including their application. Furthermore, in each work, generally only one molar ratio has been studied (1:2 or 1:3).

At first, in order to determine the general flow behaviour of our DESs, the viscosity was measured as a function of the shear rate (from 100 to 1000 s^{-1}) at 20 °C. The flow curves reported in

Fig. 4 showed a clear and typical Newtonian behaviour for all DESs. Indeed, viscosity appears constant and independent of the value and duration of the shear rate applied. However, it is worth nothing, as observed in literature for many ionic liquids [79,80] and in some cases also for DESs [81], that the most viscous solvents (Gly-containing DESs and Bet:LevA 1:2) no longer behave as Newtonian liquids at higher shear rates, but showed a decrease of the viscosity thus acquiring a shear-thinning behaviour. This behaviour indicated that DESs exist as liquid phase aggregates that can be disrupted or broken at high shear rates.

Subsequently, the viscosity of DESs was measured, applying a constant shear rate where they all behave as Newtonian liquids, increasing the temperature up to 90 °C. Data were registered with a step of 5 °C and the obtained values are reported in Tables S7–S9 and are depicted in Fig. 5. The viscosity of pure HBDs was also measured and compared to the corresponding DESs.

From the flow curves and the curves obtained as a function of temperature, it is evident that Bet-based DESs are significantly more viscous than ChCl-based DESs. Within DESs with the same HBA, the viscosity increased in the following order: EG < LevA < Gly for both ChCl and Bet-based solvents. This is in agreement with previous works that showed very low viscosities for several EG-containing DESs with different ammonium and phosphonium salts as HBA (always < 200 $\text{mPa}\cdot\text{s}$) [82] and high viscosities for various Gly-containing DESs and similar HBA [35]. Moreover, compared to pure HBDs, all EG and LevA-containing DESs showed higher viscosity than the pure constituting components. Instead, ChCl:Gly DESs were less viscous than Gly, while the opposite trend was observed for the Bet:Gly DESs. Finally, by increasing the molar ratio from 1:2 to 1:4 the viscosity decreased, with the exception of ChCl:Gly systems. Regarding trends of viscosity as a function of the temperature, a significant decrease at higher temperatures was observed in all cases. The differences between DESs at different molar ratios drastically reduced at the highest temperatures applied and, in some cases, very similar values were obtained. Our viscosity measurements showed satisfactory agreement with those available in the literature.

As for density data, the observed trends can be ascribed to the nature (molecular weight and molecular size) of HBA and HBD and hence their intermolecular interactions (hydrogen bonds, van der Waals interactions...); these parameters can greatly influence the mobility of the whole system [6]. The addition of one —OH (Gly) or —COOH (LevA) functional group with respect to EG contribute to the increase of viscosity. Again, also the hole theory can be brought into play to rationalize the results. Abbott and co-workers applied this theory showing how the presence of holes in the liquid facilitates the mobility of compounds in the final network [83]. They asserted that volumetric factors, that consider also steric effects, strongly affected the viscosity rather than the intermolecular interactions between HBA and HBD. Indeed, the distribution of the size of holes depends strictly upon the nature of both HBA and HBD. This theory well explains the decrease of viscosity as temperature increases. Holes with different size and location are in continuous motion. At lower temperatures the size of holes is small compared to the size of the DES components, which thus difficultly fit into the holes, reducing the free mobility of components and increasing the viscosity of the system [6]. Conversely, at high temperatures the average size of holes becomes comparable to the size of DES components that can easily move through holes and increase the mobility of the DES [6].

As shown, the dependence of viscosity from temperature was non-linear and this behaviour has been extensively described by the logarithmic form of the Arrhenius equation:

$$\ln \eta = \ln \infty + \frac{E_a}{RT} \quad (4)$$

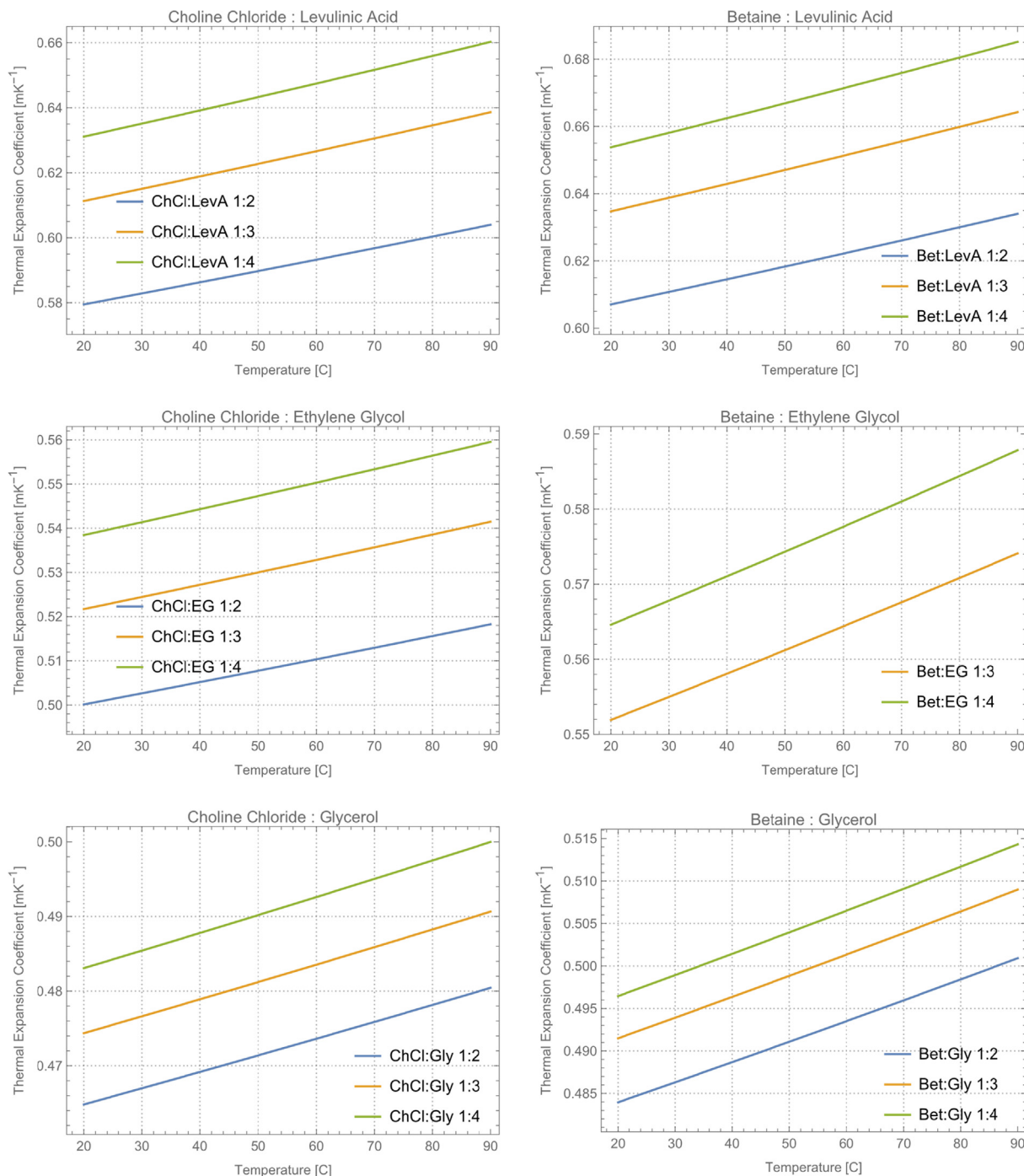


Fig. 2. Thermal expansion coefficient dependence on temperature according to (Eq. (1)) for the indicated DES and molar ratio.

where $\ln \eta_\infty$ is the viscosity at infinite temperature, E_a is the activation energy for viscosity flows and R is the ideal gas constant. The E_a was calculated from the slope of $\ln \eta$ vs $1/T$ as shown in the graphs in the supplementary file (Figs. S7–S23). The fitting parameters are reported in Table 3. The obtained data showed, in accordance with the literature [6,84], low values of E_a for less viscous DESs, with the lowest value for ChCl:EG. The most viscous DESs such as the Gly-containing ones displayed instead higher E_a with the highest one observed for Bet:Gly. LevA-containing DESs exhibited intermediate values of viscosity and consequently of E_a . Hence, calculated data of E_a perfectly correlate with the measured values of viscosity. However,

although data seem to fit well enough with the Arrhenius model, resulting R^2 for all DESs and the presence of a subtle but visible deviation from linearity in the graphs obtained by the application of selected fitting model (Figs. S7–S23) call for the adoption of a better model.

For this reason, the viscosity data were also fitted with the alternative most widely used approach to correlate the viscosity with the temperature, the Vogel-Fulcher-Tammann (VFT) model. The VFT equation is similar to the Arrhenius one, but with a substantial difference in the term $(T - T_0)$:

$$= \infty \cdot e^{\frac{B}{T-T_0}} \tag{5}$$

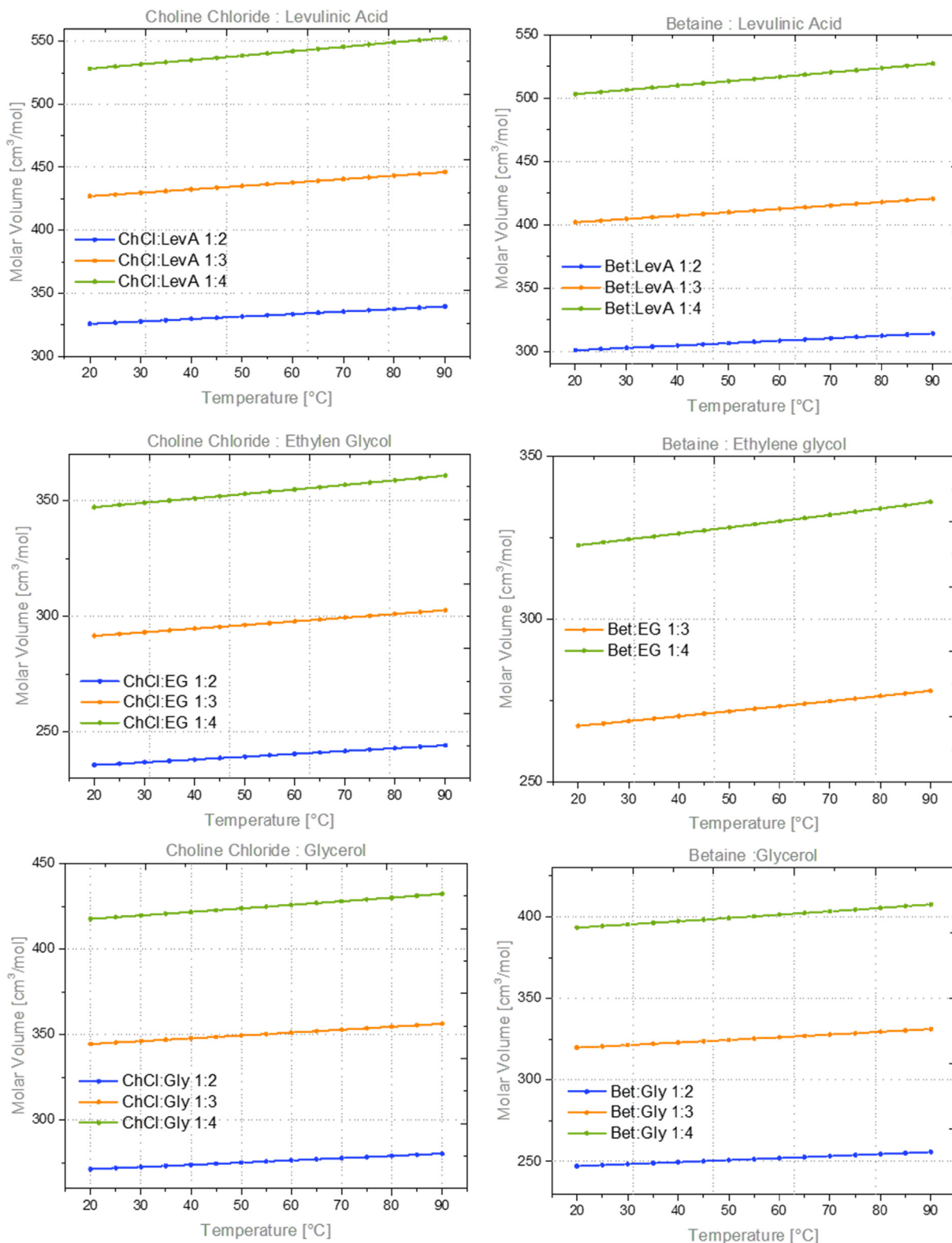


Fig. 3. Molar Volumes as a function of temperature of indicated DES and molar ratio.

where represents again the viscosity at infinite temperature and B and T_0 are fitting parameters.

The graphs of the fitting of viscosity according to the VFT model are reported in Figs. S7–S23 while the obtained fitting parameters are summarized in Table 4. The R^2 values and the fitting lines reported in the graphs, compared to the data obtained adopting the Arrhenius model, showed that the VFT approach provides an

excellent fitting for our collected experimental viscosity data (for all DESs $R^2 > 0.999$).

3.4. Refractive index

The refractive index is an important physical property in the optical characterization of materials because of the accurate and

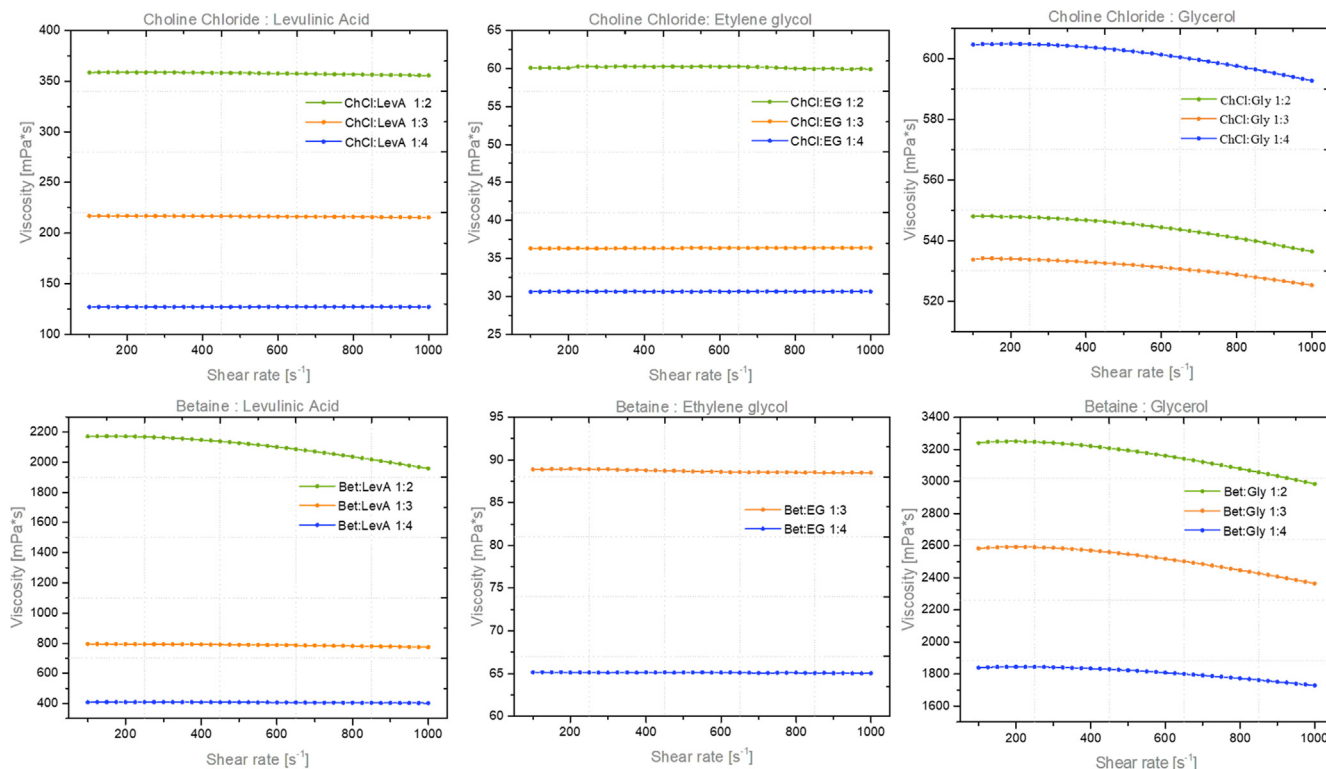


Fig. 4. Flow curves as a function of the shear rate of the indicated DES and molar ratio.

relatively straightforward experimental methods used to determine it. It also relates by well-established physical laws to other physical properties which can be independently measured, such as density and surface tension, providing a testbed for building (semi)empirical models and checking for the consistency of experimental data.

Except for the structure of the material itself, which makes the refractive index so suitable for optical characterization after all, the main factors influencing the refractive index are the material's temperature and the wavelength of incident light. While temperature effects are appreciated and often systematically investigated in the relevant literature, data regarding wavelength effects are totally absent. In some cases, the wavelength of the monochromatic light that was used to measure the refractive index, normally the standard D-line of sodium at 589.3 nm, is not even reported explicitly and must be inferred indirectly by the type of instrument used.

Systematic investigations of temperature effects on the refractive index of ChCl-based DESs with EG and Gly for various molar ratios have been carried out by many of the groups that reported density measurements [36,37,40,53,55,56]. The same holds true for ChCl-based DESs with LevA [44,57,58] and Bet-based DESs with LevA [60]. Data for the temperature dependence of the refractive index for Bet-based DESs with EG and Gly have been reported only for the 1:3 molar ratio by one of the groups that investigated the temperature dependence of density [41].

The refractive index of the DESs investigated in this work was measured for five wavelengths (450 nm, 532 nm, 633 nm, 964 nm, 1551 nm) each for temperatures from 30 °C to 100 °C. We fit the collected refractive index datasets to a nonlinear Sellmeier model of the form

$$n(\lambda, T) = \left[1 + \frac{(s_1 + s_2 T)\lambda^2}{\lambda^2 - \lambda_{uv}^2} + s_3 \lambda^2 \right]^{1/2} \quad (6)$$

which captures both wavelength and temperature dependence using four free parameters, whose optimal values are tabulated in Table 5 for each DES and molar ratio. The same Sellmeier model was used in previous work on ionic liquids with good results [47]. Fit quality is best described by the adjusted R^2 value, which also accounts for the number of independent variables in the model.

Fit quality was excellent for all DESs studied in this work, with the resulting adjusted R^2 so close to unity that it makes more sense to refer to the difference $1 - \text{adj.}R^2$, which was always less than 10^{-6} except for ChCl:LevA 1:4 where it obtained the highest value 1.58×10^{-6} .

Extrapolating the Sellmeier model outside the measured wavelength range is known to produce wrong estimates, the most absurd being the infinite refractive index when $\lambda \rightarrow \lambda_{uv}$. However, reasonable extrapolations outside the measured temperature range should be reliable and perfectly fine if no critical or phase change temperature is nearby or crossed.

Optical properties like temperature dispersion and chromatic dispersions can be ultimately determined by the derivatives of the Sellmeier model. The derivative with respect to temperature is commonly referred to as the thermo-optic coefficient and it is given by

$$\frac{\partial n}{\partial T} = \frac{s_2}{2n(\lambda, T)} \cdot \frac{\lambda^2}{\lambda^2 - \lambda_{uv}^2} \quad (7)$$

while the derivative with respect to wavelength is

$$\frac{\partial n}{\partial \lambda} = \frac{\lambda}{n(\lambda, T)} \cdot \left[s_3 - \frac{(s_1 + s_2 T)\lambda_{uv}^2}{(\lambda^2 - \lambda_{uv}^2)^2} \right] \quad (8)$$

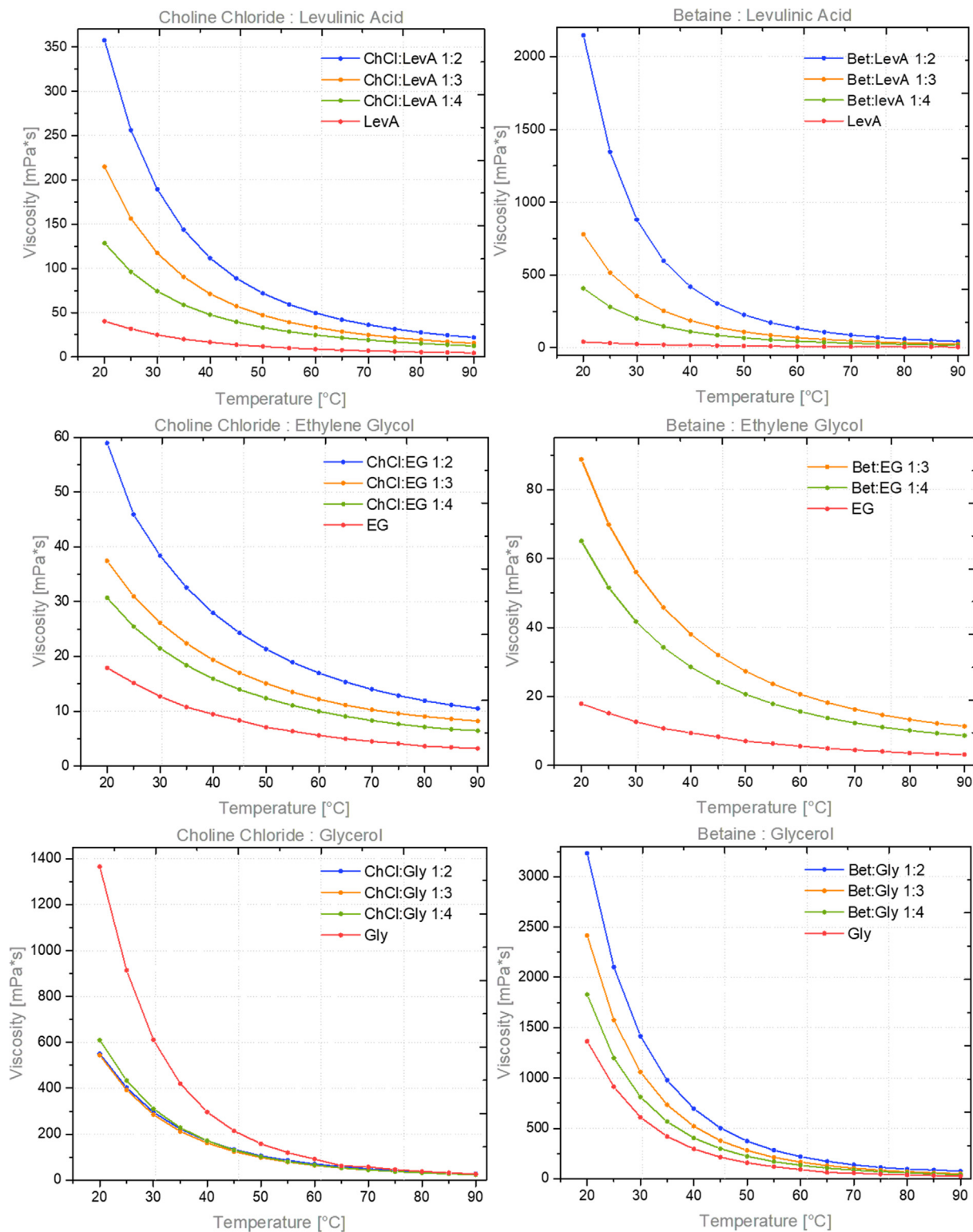


Fig. 5. Viscosity dependence on temperature for the indicated DES and molar ratio.

Chromatic dispersions of the first and second order can be expressed in terms of the group index n_g that regulates the group velocity $v_g = c/n_g$, and the dispersion of group velocity, respectively [47].

To better appreciate the behavior of the Sellmeier model for the studied DESs, Fig. 6 presents the temperature dependence at

633 nm, while Fig. 7 presents a typical wavelength dependence at 70 °C (midway between 30 °C and 100 °C).

The first striking feature of temperature dependence in all plots of Fig. 6 is its apparent linearity even though $n(T)$ is not linear in the Sellmeier model (the dielectric constant is $\epsilon = n^2$). A linear decrease of the refractive index for increasing temperatures is

Table 3

Optimal parameters of the Arrhenius model for the temperature dependence of density from 20 °C to 90 °C, for the indicated DES and molar ratio.

| DES | Molar ratio | R^2 | $\ln\eta_\infty$ | η_∞ | E_a [KJ/mol] |
|-----------|-------------|---------|------------------|----------------------|----------------|
| ChCl:LevA | 1:2 | 0.98954 | -8.56352 | $1.91 \cdot 10^{-4}$ | 34.74650 |
| ChCl:LevA | 1:3 | 0.98874 | -8.20438 | $2.73 \cdot 10^{-4}$ | 32.63935 |
| ChCl:LevA | 1:4 | 0.98812 | -7.09573 | $8.29 \cdot 10^{-4}$ | 28.70874 |
| ChCl:EG | 1:2 | 0.98648 | -4.80488 | $8.19 \cdot 10^{-3}$ | 21.29136 |
| ChCl:EG | 1:3 | 0.98269 | -4.35229 | $1.29 \cdot 10^{-2}$ | 19.14803 |
| ChCl:EG | 1:4 | 0.98833 | -4.78772 | $8.33 \cdot 10^{-3}$ | 19.76086 |
| ChCl:Gly | 1:2 | 0.99483 | -9.38438 | $8.40 \cdot 10^{-5}$ | 37.93102 |
| ChCl:Gly | 1:3 | 0.99735 | -10.00169 | $4.53 \cdot 10^{-5}$ | 39.39392 |
| ChCl:Gly | 1:4 | 0.99465 | -10.5819 | $2.54 \cdot 10^{-5}$ | 41.06686 |
| Bet:LevA | 1:2 | 0.98901 | -12.5574 | $3.52 \cdot 10^{-6}$ | 48.66027 |
| Bet:LevA | 1:3 | 0.98983 | -11.08405 | $1.54 \cdot 10^{-5}$ | 42.68056 |
| Bet:LevA | 1:4 | 0.98922 | -10.18157 | $3.79 \cdot 10^{-5}$ | 38.95268 |
| Bet:EG | 1:3 | 0.99002 | -6.24338 | $1.94 \cdot 10^{-3}$ | 25.83872 |
| Bet:EG | 1:4 | 0.99059 | -6.3562 | $1.74 \cdot 10^{-3}$ | 25.37597 |
| Bet:Gly | 1:2 | 0.98882 | -11.75165 | $7.88 \cdot 10^{-6}$ | 47.79510 |
| Bet:Gly | 1:3 | 0.99377 | -12.43044 | $4.00 \cdot 10^{-6}$ | 48.81080 |
| Bet:Gly | 1:4 | 0.99283 | -12.07827 | $5.68 \cdot 10^{-6}$ | 47.25378 |

Table 4

Optimal parameters of the VFT model for the temperature dependence of density from 20 °C to 90 °C, for the indicated DES and molar ratio.

| DES | Molar ratio | R^2 | η_∞ [mPa*s] | B [K] | T_0 [K] |
|-----------|-------------|---------|-----------------------|------------|-----------|
| ChCl:LevA | 1:2 | 0.99999 | 0.54495 | 544.92234 | 201.28465 |
| ChCl:LevA | 1:3 | 0.99999 | 0.54883 | 527.74627 | 204.60236 |
| ChCl:LevA | 1:4 | 0.99999 | 0.874 | 403.82901 | 212.08777 |
| ChCl:EG | 1:2 | 0.99952 | 1.66871 | 266.82401 | 217.98069 |
| ChCl:EG | 1:3 | 0.99971 | 1.28464 | 275.30568 | 211.45271 |
| ChCl:EG | 1:4 | 0.99989 | 0.75058 | 344.35321 | 200.24586 |
| ChCl:Gly | 1:2 | 0.99993 | 0.08854 | 1134.22196 | 163.18723 |
| ChCl:Gly | 1:3 | 0.99993 | 0.06156 | 1180.79078 | 163.08736 |
| ChCl:Gly | 1:4 | 0.99994 | 0.0476 | 1224.46717 | 163.57598 |
| Bet:LevA | 1:2 | 0.99999 | 0.21317 | 858.58387 | 199.86291 |
| Bet:LevA | 1:3 | 1 | 0.30017 | 706.60036 | 203.12556 |
| Bet:LevA | 1:4 | 0.99999 | 0.29096 | 659.48135 | 202.00513 |
| Bet:EG | 1:3 | 0.99996 | 0.59497 | 490.5073 | 195.0367 |
| Bet:EG | 1:4 | 0.99994 | 0.42848 | 511.19562 | 191.25926 |
| Bet:Gly | 1:2 | 0.99997 | 0.09816 | 1201.10752 | 177.53849 |
| Bet:Gly | 1:3 | 0.99999 | 0.05793 | 1264.47603 | 174.14742 |
| Bet:Gly | 1:4 | 0.99999 | 0.08718 | 1117.99733 | 180.65983 |

Table 5Optimal parameters of (Eq. (6)) for the indicated DES and molar ratio when λ is in nm and T in °C.

| DES | Molar Ratio | s_1 | $-10^4 s_2$ | $-10^9 s_3$ | λ_{uv} |
|-----------|-------------|---------|-------------|-------------|----------------|
| ChCl:LevA | 1:2 | 1.13406 | 7.65319 | 2.06576 | 107.266 |
| | 1:3 | 1.11638 | 7.94600 | 2.34020 | 107.009 |
| | 1:4 | 1.13510 | 10.7287 | 2.55830 | 106.352 |
| ChCl:EG | 1:2 | 1.13450 | 5.92885 | 3.00991 | 104.747 |
| | 1:3 | 1.11878 | 6.77491 | 3.37535 | 103.928 |
| | 1:4 | 1.10275 | 6.86581 | 3.22467 | 103.509 |
| ChCl:Gly | 1:2 | 1.18155 | 6.46007 | 3.31255 | 104.756 |
| | 1:3 | 1.17364 | 6.39347 | 4.55002 | 102.542 |
| | 1:4 | 1.16496 | 5.80371 | 4.03464 | 101.932 |
| Bet:LevA | 1:2 | 1.12558 | 7.86075 | 3.63414 | 105.159 |
| | 1:3 | 1.11181 | 8.24163 | 3.59010 | 104.062 |
| | 1:4 | 1.10278 | 8.42562 | 3.73152 | 104.213 |
| Bet:EG | 1:3 | 1.10469 | 7.23091 | 3.82163 | 101.351 |
| | 1:4 | 1.09146 | 7.23411 | 4.45306 | 100.822 |
| Bet:Gly | 1:2 | 1.17571 | 6.74134 | 4.87115 | 100.596 |
| | 1:3 | 1.16849 | 6.86825 | 4.63414 | 100.182 |
| | 1:4 | 1.16672 | 7.00495 | 5.32526 | 99.6437 |

commonly observed in ionic liquids and has been also reported by all groups with published data for the DES families studied in this work. It is obvious from Fig. 6 that the Sellmeier model still captures the linear evolution in the studied temperature range well, despite the assumption of $T^{1/2}$ dependence.

Another striking feature of the refractive index plots in Fig. 6 is the qualitative resemblance to the density plots presented in Fig. 1

regarding the observed linear decrease. Even the crossing of the density curves of ChCl:LevA at approximately 55 °C is observed in the refractive index curves shifted about 10 °C higher. But there are also differences, the most obvious being that the refractive index decreases when the molar ratio of the hydrogen bond donor increases, in contrast to density and the thermal expansion coefficient, which exhibit the exact opposite behavior. It is also the case

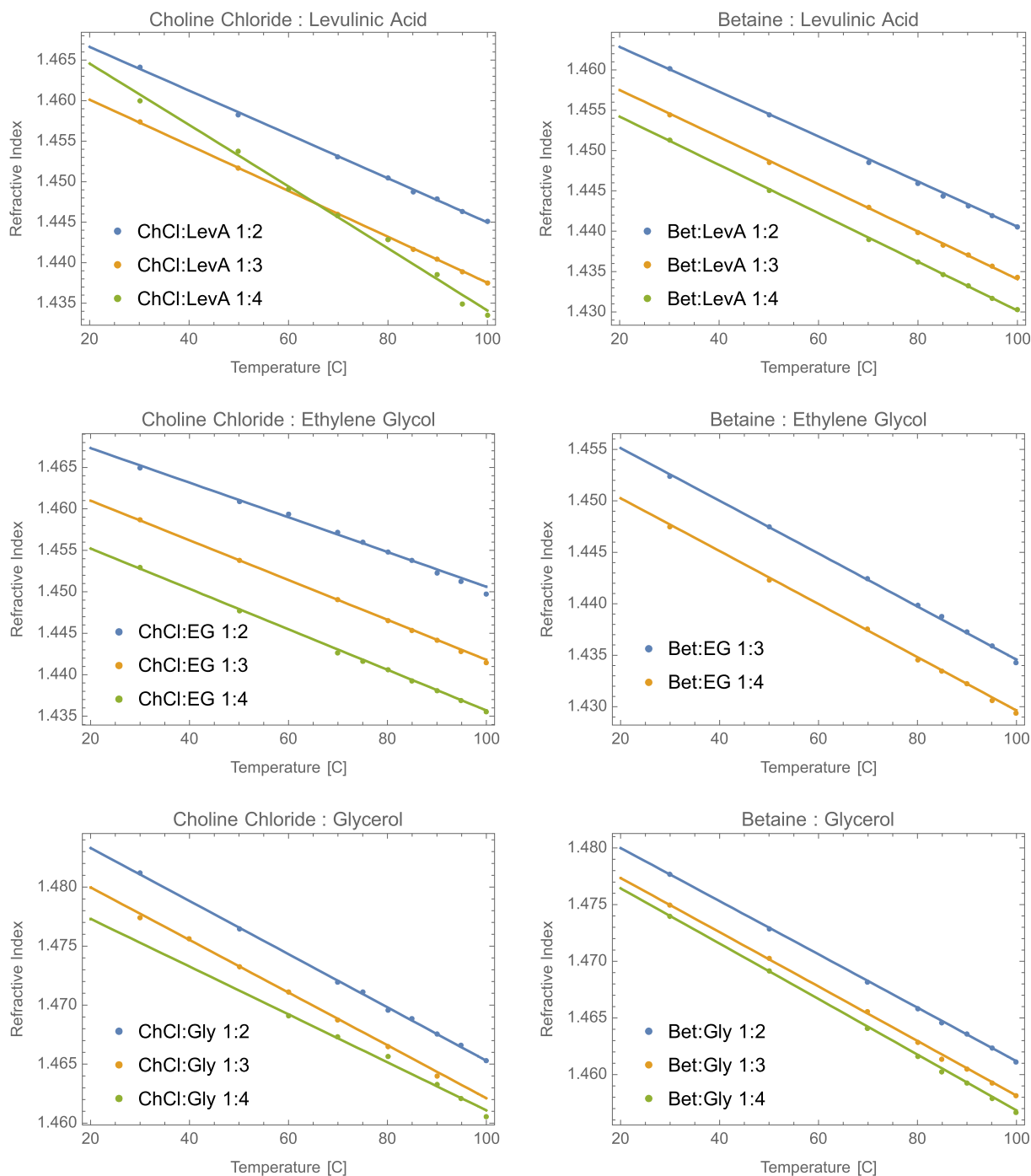


Fig. 6. DES refractive index dependence on wavelength for different molar ratios at 633 nm. Dots are measurements, while solid curves are the corresponding Sellmeier model fits with the parameters of Table 5.

that the refractive index is increasing in the order ChCl > Bet with respect to the hydrogen bond acceptor instead of the opposite order encountered in the density data. However, in contrast to density and the thermal expansion coefficient, there is no clear order of increase or decrease of the refractive index in terms of the HBD (LevA, EG, Gly) for the same molar ratio and HBA.

The typical wavelength dependence from 450 nm to 1551 nm of the refractive index at 70 °C, a temperature lying roughly in the middle of the measured temperature range, is shown in Fig. 7. In accordance with the Sellmeier model, the refractive index is monotonically decreasing toward the infrared part of the spectrum at a progressively lower rate, and there are no curve crossings in

general. Indeed, the very small refractive index difference between ChCl:LevA 1:3 and ChCl:LevA 1:4 at 70 °C visible in Fig. 6 is carried over throughout the measured wavelength range.

3.5. Physical models relating density and the refractive index

An important physical property related to the atomic polarizability is molar refractivity, usually denoted by R_m . Molar refractivity depends on both density and the refractive index, as dictated by the Clausius-Mossotti (or, sometimes, Lorenz-Lorentz) equation

$$R_m = \frac{M_w}{\rho} \frac{n^2 - 1}{n^2 + 2} \quad (9)$$

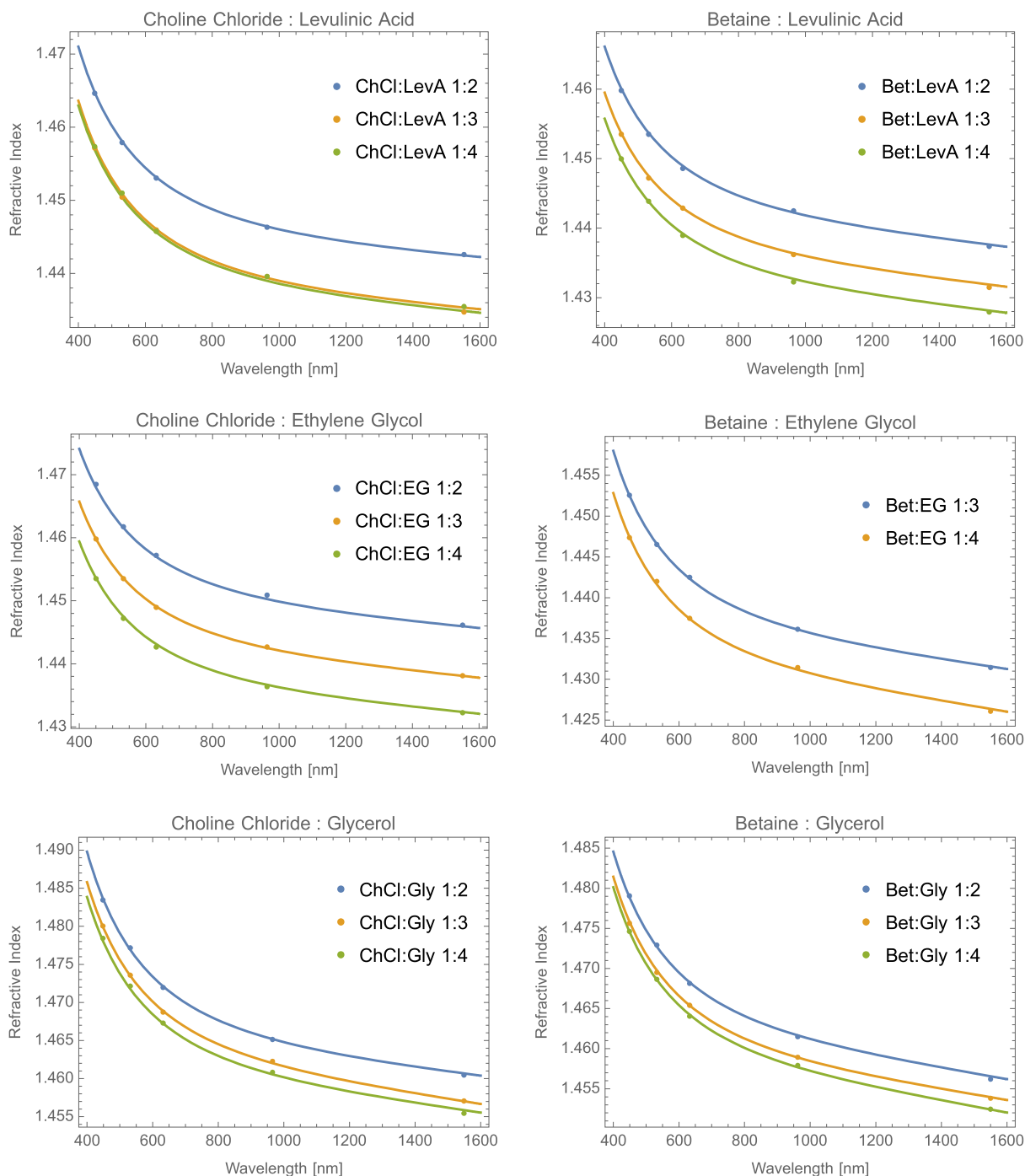


Fig. 7. DES refractive index dependence on wavelength for different molar ratios at 70 °C. Dots are measurements, while solid curves are the corresponding Sellmeier model fits with the parameters of Table 5.

In the equation above, M_w is the molar mass, ρ is the density and n the refractive index. When data on density and the refractive index of a substance are available, one can determine molar refractivity at a given temperature and wavelength (usually the D-line of sodium at 589.3 nm).

On the other hand, the large number of density and refractive index data collected over the years for many compounds, made possible the development of semiempirical models for predicting the molar refractivity of a substance. The Wildman-Crippen model [85] takes advantage of the additivity of molar refractivity by defining atomic contributions to molar refractivity for specific chemical elements. A distinguishing feature of the model is that

it assigns different contributions to certain chemical elements (carbon, hydrogen, nitrogen, oxygen) depending on what other elements or functional groups bond with them in the molecule under consideration. Total molar refractivity is the sum of individual contributions $[MR]_i$, while accounting for k_i appearances of the i -th type of atom in the molecule,

$$R_m = \sum_i k_i [MR]_i \quad (10)$$

Since the DESs in this work are binary mixtures of HBA and HBD with a molar ratio of 1 : r , the molar refractivity of the DES should be simply

$$R_m[\text{DES}] = \frac{1}{1+r} (R_m[\text{HBA}] + rR_m[\text{HBD}]) \quad (11)$$

This approach before applying (Eq. (9)), which takes full advantage of the additivity of molar refractivity, is also favored by other workers in the field [53]. The alternative would be to use the molar refractivity of the components and one of the many proposed mixing rules to calculate the refractive index of the DES in terms of its components. This alternative approach is obviously unworkable in our case since our measurements concern the refractive index of the final DES.

Density and refractive index data along with the molar mass of each DES, which is calculated similarly to (Eq. (11)) from the

known molar mass of its constituents while accounting for their molar ratio, can be substituted in (Eq. (9)) to obtain the molar refractivity of the respective DES. When we constrain ourselves to refractive index data at 589.3 nm for better reference with published data, the temperature dependence of molar refractivity for each DES studied in this work results in the plots of Fig. 8. Molar refractivity exhibits a weak positive temperature dependence, except for DES with LevA where this dependence is more pronounced and even negative in the case of ChCl:LevA 1:4.

The Wildman-Crippen model [85] is silent on both the temperature and wavelength dependence of molar refractivity. Since the authors of the model do not even report the temperature and

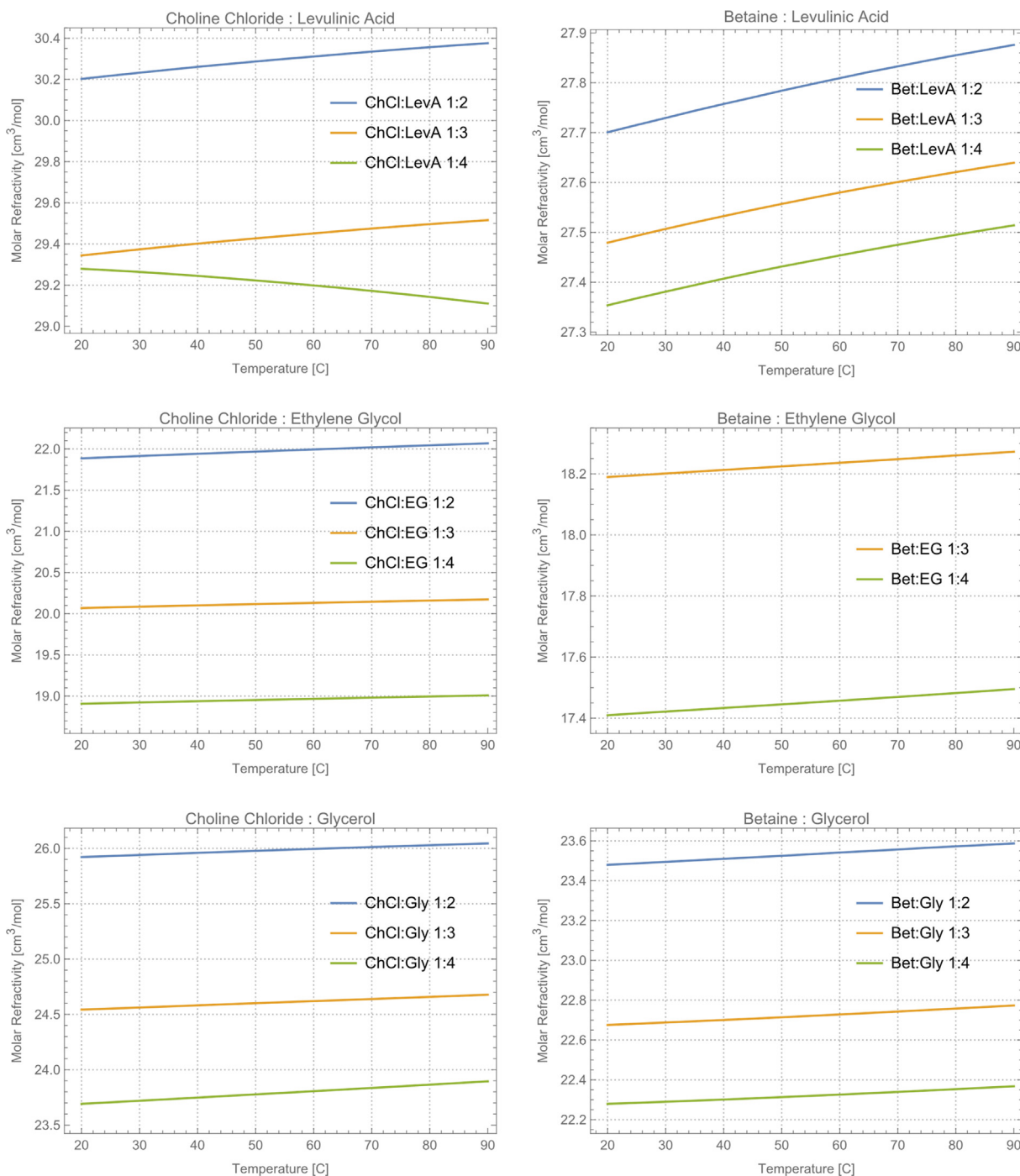


Fig. 8. DES molar refractivity dependence on temperature according to (Eq. (1)) for different molar ratios at the standard wavelength of 589.3 nm.

Table 6

Measured and predicted molar refractivities according to (Eq. (9)) and the atomic contribution model of Wildman and Crippen [85] respectively, for the indicated DES and molar ratio.

| DES | Molar Ratio | Molar Refractivity at 20 °C [cm ³ /mol] | |
|----------|-------------|--|-----------|
| | | Measured | Predicted |
| ChCl:EG | 1:2 | 21.9 | 21.4 |
| | 1:3 | 20.1 | 19.6 |
| | 1:4 | 18.9 | 18.5 |
| ChCl:Gly | 1:2 | 25.9 | 25.4 |
| | 1:3 | 24.5 | 24.1 |
| | 1:4 | 23.7 | 23.3 |

wavelength at which their proposed atomic contributions to molar refractivity are correct, we will assume a temperature of 20 °C and the standard wavelength of 589.3 nm.

The decompositions of ChCl, Gly, and EG according to the atomic types of the model do not present any problems, and the resulting molar refractivities for each molecule, 35.838, 20.178, and 14.171 respectively, are easy to calculate [53]. The predicted molar refractivity for the studied DESs containing these compounds can then be obtained from (Eq. (11)) and compared with the molar refractivity obtained by (Eq. (9)) from our density and refractive index measurements. The results, listed in Table 6, never deviate >2.2 %, indicating an excellent agreement between theory and experiment. It is immediately apparent that the predicted molar refractivities systematically underestimate the molar refractivities measured, and this shortfall has been independently observed by other workers as well [53].

Working along the same lines for DESs containing Bet and LevA, we came up with the atomic type decompositions proposed in Table 7. Due to lack of sufficient data, Wildman and Crippen could not determine a reliable molar refractivity contribution of O12 and left the relevant entry empty in their original publication [85]. The molar refractivities of Bet and LevA are then 28.295 + O12 and 27.116 + O12, where O12 is the unknown contribution of acidic oxygen.

Molar refractivities for DESs with Bet or LevA can be determined from our data, as Fig. 6 demonstrates, and those measured at 20 °C are listed in the relevant column of Table 8. The unknown contribution of O12 for each DES and molar ratio can be easily worked out from measured molar refractivities and it is also listed in Table 8. The mean value of O12 contributions can then be used as a surrogate in the Wildman-Crippen model to calculate the predicted molar refractivities in Table 8.

Even using that crude surrogate value for O12 contribution, the deviation between measured and predicted molar refractivities is never >3.6 %, a value certainly greater than the 2.2 % encountered in Table 6, though not by much. More interesting, however, is the appearance of two distinct groups in Table 8, one where O12 contribution is almost neutralized and a second, consisting of DESs with Bet and alcohols, where O12 contribution in molar refractivity is much larger. Bet:LevA DESs, both of which contain an O12 acidic

Table 7

Proposed decomposition of betaine and levulinic acid in the atomic types of the Wildman-Crippen model [85]. Molar refractivity (MR) contributions for each type are also provided for easier reference.

| | Atomic Type | | | | | | | | |
|------|-------------|-------|-------|-------|-------|--------|-------|--------|-----|
| | C1 | C3 | C5 | H1 | H4 | N13 | O9 | O11 | O12 |
| MR | 2.503 | 2.753 | 5.007 | 1.057 | 1.805 | 0.2604 | 0.000 | 0.3890 | N/A |
| Bet | 0 | 4 | 1 | 11 | 0 | 1 | 0 | 1 | 1 |
| LevA | 3 | 0 | 2 | 7 | 1 | 0 | 1 | 1 | 1 |

Table 8

Measured molar refractivities according to (Eq. (9)) and predicted O12 contributions in the atomic contribution model of Wildman and Crippen [85], for the indicated DES and molar ratio. Predicted refractivities were calculated using the mean value of the resulting O12 contributions.

| DES | Molar Ratio | Molar Refractivity at 20 °C [cm ³ /mol] | | O12 | |
|-----------|-------------|--|-----------|-----------|-------|
| | | Measured | Predicted | | |
| ChCl:LevA | 1:2 | 30.2 | 30.7 | 0.268 | |
| | 1:3 | 29.3 | 30.0 | 0.063 | |
| | 1:4 | 29.3 | 29.7 | 0.524 | |
| Bet:LevA | 1:2 | 27.7 | 28.5 | 0.192 | |
| | 1:3 | 27.5 | 28.4 | 0.068 | |
| | 1:4 | 27.4 | 28.4 | 0.002 | |
| Bet:EG | 1:3 | 18.2 | 18.0 | 1.949 | |
| | 1:4 | 17.4 | 17.2 | 2.069 | |
| | Bet:Gly | 1:2 | 23.5 | 23.2 | 1.787 |
| 1:3 | | 22.7 | 22.5 | 1.873 | |
| 1:4 | | 22.3 | 22.0 | 2.390 | |
| | | | | Mean O12: | 1.017 |

oxygen, exhibit the largest O12 neutralization among the DESs studied. Moreover, the already small O12 contribution to molar refractivity is further reduced when the molar ratio of LevA increases.

3.6. Thermal properties

Thermal properties in terms of thermal stability and thermal behavior are fundamental properties along with the rheological characteristics to evaluate any possible applications of these solvents. These properties are necessary to determine the operative range of temperature within which DESs can withstand without degradation and at the same time retain the liquid form.

3.6.1. Thermal gravimetric analysis

The short thermal stability of DESs was ascertained by employing thermal gravimetric analysis. The short thermal stability (ramped temperature analysis) along with the long thermal one (isothermal temperature analysis) is the most commonly used techniques to investigate the thermal stability of a sample [86]. While the long thermal stability is generally preferred to obtain more reliable information on the maximum operating temperature, the short thermal stability allows for performing a fast and straightforward comparison of different samples [87]. This latter technique was thus selected here to evaluate the thermal stability as a function of the solvent composition. Compared to the rheological properties, very few works reported the analyses of the thermal properties of DESs and often only decomposition temperatures (T_{dec}) have been listed without thermograms and their DTG analyses or comparison with the pure components. Regarding the DESs studied in this work, only thermal studies of ChCl:EG and ChCl:Gly DESs and in one instance of ChCl:LevA have been reported [40,88–92], while for Bet based-DESs only TGA of Bet:LevA 1:2 and Bet:Gly 1:2 were featured by Sánchez et al. [60]

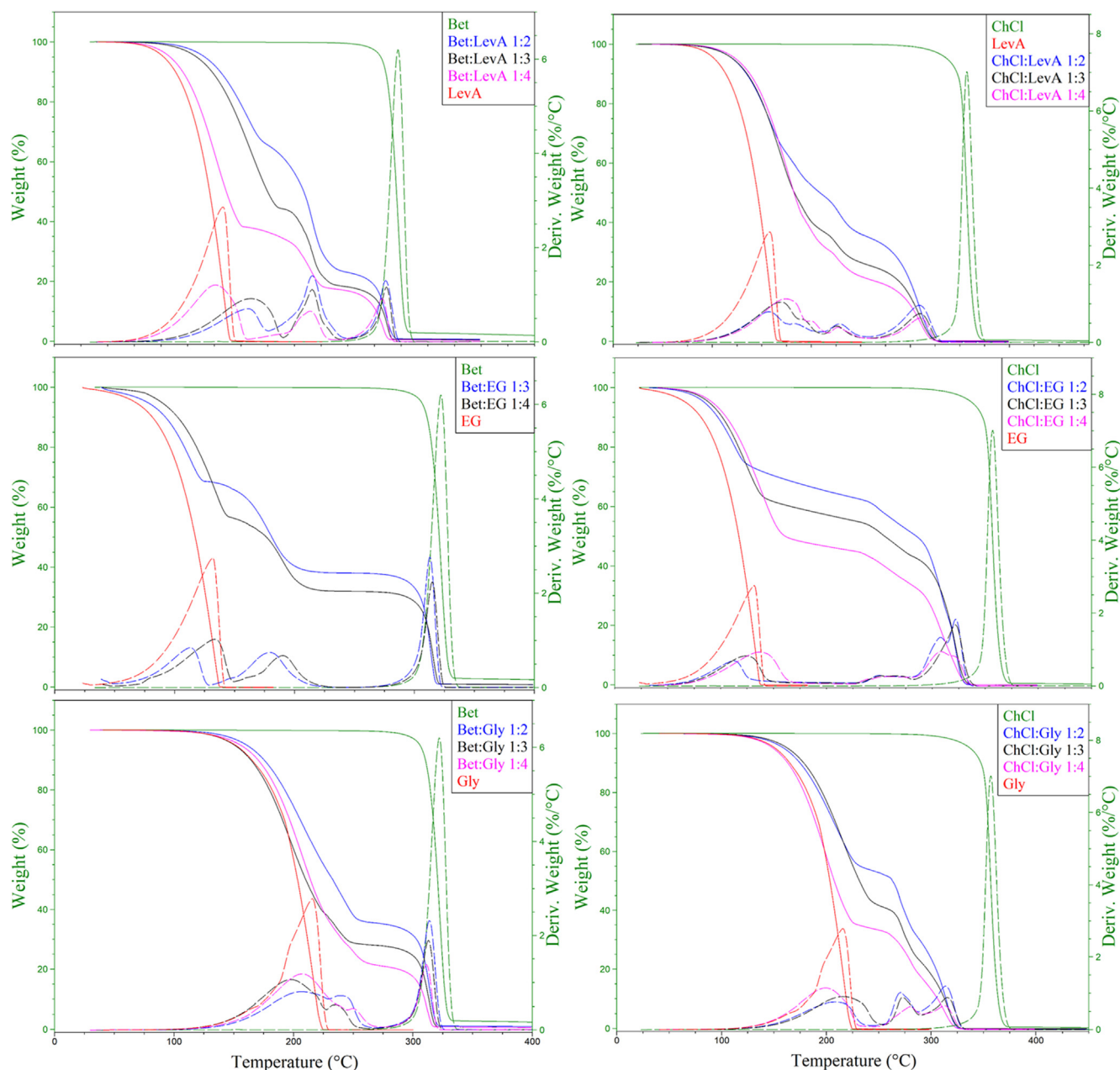


Fig. 9. TG and DTG curves of ChCl and Bet-based DESs and their components.

and Fuad and Nadzir [61]. Before carrying out the analyses, all sample have been dried (isothermal run at 60 °C for 30 min) to remove possible water absorbed from the atmosphere while their loading into the TGA pan. Afterwards, DESs were subjected at a continuous linear increase of temperature at 10 °C/min up to 500 °C and the mass loss was recorded as a function of temperature. Two characteristic values, T_{onset} and T_{peak} , denoting the thermal stability were evaluated for each sample. T_{onset} is the point of intersection between the baseline weight and the tangent of the weight against the temperature curve when decomposition of samples occurs and represents the starting degradation step, while T_{peak} , derived from the DTG curve represents the temperature at which the maximum degradation rate was observed. For comparison TG analyses were performed also on the pure HBAs and HBDs. Comparison of curves and related derivatives of both components and DESs at the three different molar ratios (1:2; 1:3; 1:4) are depicted in Fig. 9. The single thermogram of each DES is reported

in the supplementary file (Figs. S24–S40). Table 9 summarizes all the obtained values from thermograms and derivatives.

For all examined DESs there are three main peaks in the derivative curves (DTG). In any case, by comparing the curves obtained from DESs and their components, it is possible to ascribe the first significant weight loss to the HBDs evaporation/degradation and the third main peak to the HBA degradation. The intermediate peak and its relative weight loss can be attributed to both components that are strictly bonded within a hydrogen bonding network. These observations are in agreement with the results reported before in a work where thermal stability and analysis of the gases evolved during the thermal decomposition of the different DESs (some based on ChCl and EG, Gly and LevA) were evaluated by TG-FTIR analysis [92]. A similar approach (TGA/FTIR-ATR) has been reported for eight ChCl-based DESs by Delgado-Mellado et al. [90].

This study shows that the thermal stability of a DES is strictly related to the HBD when highly stable salts are used as HBA.

Indeed, as observed from the comparison of TG and DTG curves of pure components reported in Fig. S41, ChCl and Bet display a single sharp mass loss around or higher than 300 °C, while the three HBDs are much less thermally stable. Their thermal stability decreases in following order: Gly > LevA > EG. The same trend is reflected in the thermal stability of the DESs. Unsurprisingly, by increasing the molar ratio from 1:2 to 1:4, an increase of the weight loss correlated to the degradation of the HBD and a concomitant decrease of the mass loss associated to the HBA degradation was recorded. An interesting decrease of the weight loss related to the middle peak was also observed. This last difference may be explained with a less intense network of hydrogen bonds. This intermediate step of degradation may lead to a greater weight loss when the employed molar ratio is close to the eutectic point.

3.6.2. Differential scanning calorimetry

The thermal behavior of DESs was analyzed by differential scanning calorimetry. The phase behavior was explored under nitrogen atmosphere in the temperature range from –90 to 100 °C with a heating rate of 10 °C/min. The comparison of the heating runs of analyzed DESs is shown in Fig. 10, while the single thermograms comprising the heating and cooling runs are reported in the supplementary file (Figs. S42–S58). The characteristic temperatures in terms of T_g , T_m , T_c or T_{cc} are listed in Table 10. Only glass transition temperatures without any fusion events were detected for LevA-containing DESs both with Bet and ChCl as HBA and for Bet:Gly DESs at very low temperatures (below –50 °C), as it has been reported for other studied DESs

[57,60,72,93,94]. For the three mentioned families of DESs, a decrease of T_g value was observed by increasing the molar ratio from 1:2 to 1:4. This trend was particularly evident for Bet:LevA DESs. The influence of both HBA and HBD on the glass transition temperature was clear. Indeed, significant differences were detected changing ChCl with Bet when LevA was used as HBD, but also when Gly was employed instead of LevA in Bet-based DESs. For Bet:EG and ChCl:Gly DESs no thermal events were noticeable in the thermograms, suggesting that glass transitions may occur at temperatures below those detectable by our equipment. This behaviour was also observed with similar systems [95]. For instance, Jani et al. [96] reported T_g value below –100 °C for ChCl:EG 1:2. In our experiments, no T_g was observed for ChCl:EG DESs cooling down to –90 °C. At the same time only this class of DESs showed melting and crystallization events. In particular, a T_{cc} in the range of temperatures from –40 °C to –50 °C followed by a T_m around –25 °C were identified for all the three molar ratios. ChCl:EG 1:2 thermogram (Fig. S45) also displayed an evident T_c at –0.03 °C, while the T_{cc} was less intense compared to the other molar ratios where only T_{cc} was recorded. A similar behavior was reported for this solvent again by Jani et al. [96] although with different values of temperatures. This can be ascribed to the different heating and cooling rates applied and to different water content. According to these data, all DESs under investigation are ideal candidates as solvents for several applications. Indeed, they are all liquids at room temperature, and they maintain a liquid state in a very large range of temperatures.

Table 9
TGA data of all investigated DESs.

| DES | Molar ratio | TGA | | | | | |
|-----------|-------------|-------------------------------|---|-------------------------------|---|-------------------------------|---|
| | | $T_{onset1}/^{\circ}\text{C}$ | $T_{peak1}/^{\circ}\text{C}$ (Mass loss %) | $T_{onset2}/^{\circ}\text{C}$ | $T_{peak2}/^{\circ}\text{C}$ (Mass loss %) | $T_{onset3}/^{\circ}\text{C}$ | $T_{peak3}/^{\circ}\text{C}$ (Mass loss %) |
| ChCl:LevA | 1:2 | 126.05 | 157.15–183.08 (49.64) | (220.94) | 228.50 (15.20) | 289.98 | 309.13 (35.27) |
| ChCl:LevA | 1:3 | 133.52 | 169.57 (62.88) | (219.29) | 219.29 (11.58) | 291.43 | 291.43 (25.49) |
| ChCl:LevA | 1:4 | 138.10 | 174.38 (68.86) | (237.85) | 226.75 (10.51) | 293.92 | 310.20 (20.58) |
| ChCl:EG | 1:2 | 86.12 | 112.63 (31.31) | 246.07 | 250.04 (17.29) | 296.74 | 307.86–322.20 (51.23) |
| ChCl:EG | 1:3 | 94.63 | 123.88 (40.76) | 241.82 | 251.95 (15.55) | 307.07 | 321.74 (43.51) |
| ChCl:EG | 1:4 | 102.34 | 136.84 (52.99) | 237.80 | 260.53 (13.08) | 295.91 | 308.13 (33.73) |
| ChCl:Gly | 1:2 | 167.45 | 208.47 (46.26) | 263.83 | 270.74 (23.59) | (303.53) | 313.75 (30.35) |
| ChCl:Gly | 1:3 | 167.49 | 205.23 (58.55) | 260.13 | 267.29 (18.02) | 304.01 | 314.06 (23.44) |
| ChCl:Gly | 1:4 | 163.57 | 199.32 (65.16) | 266.22 | 280.21 (17.79) | (305.18) | 312.82 (16.86) |
| Bet:LevA | 1:2 | 144.72 | 180.39 (34.62) | 228.87 | 241.60 (42.43) | 302.14 | 309.75 (22.18) |
| Bet:LevA | 1:3 | 144.46 | 184.34 (55.70) | 231.17 | 241.72 (25.93) | 302.77 | 311.15 (17.76) |
| Bet:LevA | 1:4 | 119.27 | 151.03 (61.77) | 222.19 | 239.86 (20.73) | 295.66 | 307.16 (17.01) |
| Bet:EG | 1:3 | 89.66 | 112.44 (31.44) | 158.71 | 179.14 (30.30) | 303.24 | 312.12 (37.20) |
| Bet:EG | 1:4 | 101.74 | 132.69 (43.78) | 174.25 | 189.81 (24.04) | 304.81 | 314.00 (31.04) |
| Bet:Gly | 1:2 | 167.11 | 207.01 (47.96) | – | 239.65 (16.67) | 306.02 | 313.76 (34.42) |
| Bet:Gly | 1:3 | 169.87 | 206.27 (62.45) | – | 245.72 (11.51) | 303.30 | 311.36 (36.71) |
| Bet:Gly | 1:4 | 171.50 | 207.36 (71.45) | – | 249.75 (7.689) | 303.5 | 311.38 (20.16) |

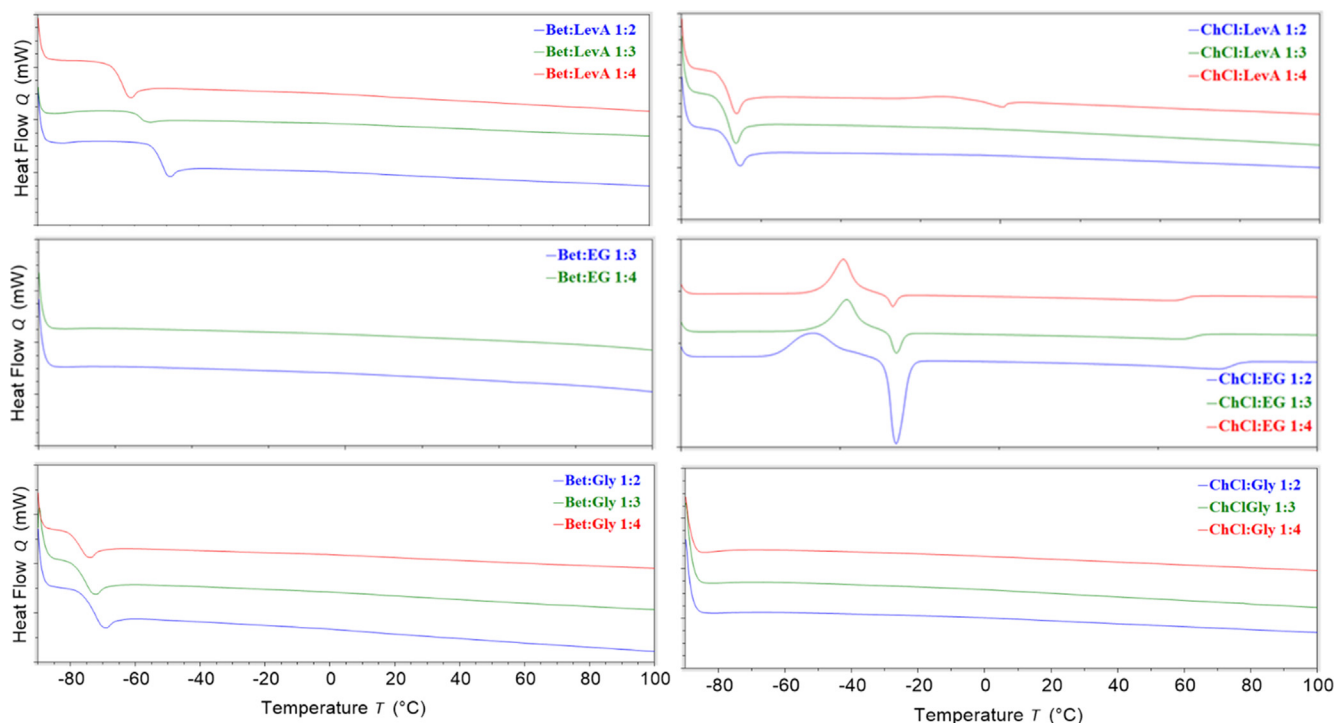


Fig. 10. DSC thermograms (heating runs from $-90\text{ }^{\circ}\text{C}$ to $100\text{ }^{\circ}\text{C}$) of all DESs at different molar ratio.

Table 10

DSC data of all DESs at the different molar ratio.

| DES | Molar ratio | DSC | | | |
|-----------|-------------|------------------------------|------------------------------|------------------------------|---------------------------------|
| | | T_g ($^{\circ}\text{C}$) | T_m ($^{\circ}\text{C}$) | T_c ($^{\circ}\text{C}$) | T_{cc} ($^{\circ}\text{C}$) |
| ChCl:LevA | 1:2 | -76.06 | - | - | - |
| ChCl:LevA | 1:3 | -77.20 | - | - | - |
| ChCl:LevA | 1:4 | -77.12 | - | - | - |
| ChCl:EG | 1:2 | - | -25.80 | -0.03 | -50.59 |
| ChCl:EG | 1:3 | - | -25.63 | - | -40.67 |
| ChCl:EG | 1:4 | - | -26.77 | - | -41.53 |
| ChCl:Gly | 1:2 | - | - | - | - |
| ChCl:Gly | 1:3 | - | - | - | - |
| ChCl:Gly | 1:4 | - | - | - | - |
| Bet:LevA | 1:2 | -52.70 | - | - | - |
| Bet:LevA | 1:3 | -59.06 | - | - | - |
| Bet:LevA | 1:4 | -65.03 | - | - | - |
| Bet:EG | 1:3 | - | - | - | - |
| Bet:EG | 1:4 | - | - | - | - |
| Bet:Gly | 1:2 | -74.09 | - | - | - |
| Bet:Gly | 1:3 | -76.62 | - | - | - |
| Bet:Gly | 1:4 | -78.23 | - | - | - |

4. Conclusions

The physicochemical properties of some DESs based on choline chloride and betaine as HBA and ethylene glycol, glycerol and levulinic acid as HBD have been experimentally determined and compared. In particular, rheological, optical and thermal properties have been analyzed at different temperatures as a function of HBA/HBD composition and their molar ratio. EG-based DESs displayed the lowest density and viscosity values and ChCl:EG 1:4 represented the less dense and viscous system. Conversely, Gly-based DESs exhibited the highest values of both density and viscosity and, among them, Bet:Gly 1:4 was the most dense and viscous DES. All LevA-based DESs showed an intermediate behavior. For DESs containing the same HBD, all Bet-based DESs appeared more viscous and dense compared to those based on ChCl as HBA.

Moreover, increasing the molar ratio caused a decrement of viscosity for all DESs studied, while a different behaviour was observed concerning density. Indeed, an increase of density was observed for all Gly-based DESs, while a decrement was found for EG and LevA-based DES. Finally, both density and viscosity decreased with temperature in the case of all DESs studied. In particular, the density values decreased linearly while the decrease of viscosity as a function of temperature showed the best fitting parameters according to the VFT model. The observed trends of density and viscosity can be ascribed to the nature (molecular weight, molecular size and the presence of different functional groups such as $-\text{OH}$ or $-\text{COOH}$) of the HBA and HBD components and hence their capacity to establish intermolecular interactions through hydrogen bonds. These have a large influence on the number of free volumes, holes and the mobility of the whole system. The

trend between refractive index, temperature and wavelength follows the behavior described by the Sellmeier model. Increasing the relative amount of the HBD component compared to the HBA generally led to a decrease in the refractive index at the studied temperature and wavelength range with the exception of ChCl:LevA. In this particular instance, the reverse trend is observed at temperatures higher than 65 °C and for molar ratios 1:3 and 1:4. The molar refractivity calculated by the Clausius-Mossotti equation using experimentally obtained data on density and refractive index is consistent with the one predicted by the well-established Wildman-Crippen model.

The thermal properties showed that the stability of all investigated DESs is strictly related to the HBD portion, for which the trend is EG < LevA < Gly. As a result, the EG-containing DESs were less stable than those containing LevA, while Gly-based DESs were the most stable DESs. Moreover, three characteristic mass loss steps were present in all the studied DESs. They can be attributed to the HBD portion, to the strongly interacting HBD-HBA system and to the HBA evaporation/degradation events, respectively. Analysis of the thermal behavior showed a glass transition only in a relatively number of cases and at low temperatures, especially when the molar ratio was increased from 1:2 to 1:4 for LevA-containing DESs with both Bet and ChCl as HBA and for Bet:Gly DESs. Instead, for Bet:EG and ChCl:Gly DESs, no thermal events were observed. Lastly, all ChCl:EG DESs displayed a clear melting event around -20 °C, preceded by a cold crystallization event. These results showed that all DESs presented in this work can potentially substitute conventional solvents by virtue of their being liquid at room temperature and due to the ability to maintain their liquid state across a broad range of temperatures.

Data availability

Data will be made available on request.

Declaration of Competing Interest

The authors declare that they have no known competing financial interests or personal relationships that could have appeared to influence the work reported in this paper.

Appendix A. Supplementary material

Supplementary data to this article can be found online at <https://doi.org/10.1016/j.molliq.2023.121563>.

¹H NMR spectra, tables of density, molar volume and viscoisty values, fitting of viscosity data, TG and DTG curves, and DSC curves.

References

- [1] A.P. Abbott, G. Capper, D.L. Davies, R.K. Rasheed, V. Tambyrajah, Novel solvent properties of choline chloride/urea mixtures, *Chem. Commun.* (2003) 70–71, <https://doi.org/10.1039/b210714g>.
- [2] M.A.R. Martins, S.P. Pinho, J.A.P. Coutinho, Insights into the nature of eutectic and deep eutectic mixtures, *J. Solution Chem.* 48 (2019) 962–982, <https://doi.org/10.1007/s10953-018-0793-1>.
- [3] B.B. Hansen, S. Spittle, B. Chen, D. Poe, Y. Zhang, J.M. Klein, A. Horton, L. Adhikari, T. Zelovich, B.W. Doherty, B. Gurkan, E.J. Maginn, A. Ragauskas, M. Dadmun, T.A. Zawodzinski, G.A. Baker, M.E. Tuckerman, R.F. Savinell, J.R. Sangoro, Deep eutectic solvents: a review of fundamentals and applications, *Chem. Rev.* (2020), <https://doi.org/10.1021/acs.chemrev.0c00385>.
- [4] Y. Liu, J.B. Friesen, J.B. McAlpine, D.C. Lankin, S.-N. Chen, G.F. Pauli, Natural deep eutectic solvents: properties, applications, and perspectives, *J. Nat. Prod.* 81 (2018) 679–690, <https://doi.org/10.1021/acs.jnatprod.7b00945>.
- [5] T. El Achkar, H. Greige-Gerges, S. Fourmentin, Basics and properties of deep eutectic solvents: a review, *Environ. Chem. Lett.* 19 (2021) 3397–3408, <https://doi.org/10.1007/s10311-021-01225-8>.
- [6] S.P. Ijardar, V. Singh, R.L. Gardas, Revisiting the physicochemical properties and applications of deep eutectic solvents, *Molecules* 27 (2022) 1368, <https://doi.org/10.3390/molecules27041368>.
- [7] M. Shaibuna, L.V. Theresa, K. Sreekumar, Neoteric deep eutectic solvents: history, recent developments, and catalytic applications, *Soft Matter* 18 (2022) 2695–2721, <https://doi.org/10.1039/D1SM01797G>.
- [8] G. Colombo Dugoni, A. Sacchetti, A. Mele, Deep eutectic solvent as solvent and catalyst: one-pot synthesis of 1,3-dinitropropanes via tandem Henry reaction/Michael addition, *Org. Biomol. Chem.* 18 (2020) 8395–8401, <https://doi.org/10.1039/D00B01516D>.
- [9] S. Arnaboldi, A. Mezzetta, S. Grecchi, M. Longhi, E. Emanuele, S. Rizzo, F. Arduini, L. Micheli, L. Guazzelli, P.R. Mussini, Natural-based chiral task-specific deep eutectic solvents: a novel, effective tool for enantiodiscrimination in electroanalysis, *Electrochim. Acta* 380 (2021), <https://doi.org/10.1016/j.electacta.2021.138189>.
- [10] J.K.U. Ling, K. Hadinoto, Deep eutectic solvent as green solvent in extraction of biological macromolecules: a review, *Int. J. Mol. Sci.* 23 (2022) 3381, <https://doi.org/10.3390/ijms23063381>.
- [11] L.B. Santos, R.S. Assis, J.A. Barreto, M.A. Bezerra, C.G. Novaes, V.A. Lemos, Deep eutectic solvents in liquid-phase microextraction: contribution to green chemistry, *TrAC Trends Anal. Chem.* 146 (2022), <https://doi.org/10.1016/j.trac.2021.116478>.
- [12] A. Delavault, K. Ochs, O. Gorte, C. Syltatk, E. Durand, K. Ochsenreither, Microwave-assisted one-pot lipid extraction and glycolipid production from oleaginous yeast *Saitozyma podzolica* in sugar alcohol-based media, *Molecules* 26 (2021) 470, <https://doi.org/10.3390/molecules26020470>.
- [13] J. Gonzalez-Rivera, C. Duce, B. Campanella, L. Bernazzani, C. Ferrari, E. Tanzini, M. Onor, I. Longo, J.C. Ruiz, M.R. Tinè, E. Bramanti, In situ microwave assisted extraction of clove buds to isolate essential oil, polyphenols, and lignocellulosic compounds, *Ind. Crop. Prod.* 161 (2021), <https://doi.org/10.1016/j.indcrop.2020.113203>.
- [14] H. Moni Bottu, A. Mero, E. Husanu, S. Tavernier, C.S. Pomelli, A. Dewaele, N. Bernaert, L. Guazzelli, L. Brennan, The ability of deep eutectic solvent systems to extract bioactive compounds from apple pomace, *Food Chem.* 386 (2022), <https://doi.org/10.1016/j.foodchem.2022.132717>.
- [15] X. Shang, Y. Zhang, Y. Zheng, Y. Li, Temperature-responsive deep eutectic solvents as eco-friendly and recyclable media for microwave extraction of flavonoid compounds from waste onion (*Allium cepa* L.) skins, *Biomass Convers. Biorefin.* (2022), <https://doi.org/10.1007/s13399-022-02483-4>.
- [16] F.S. Costa, L.S. Moreira, A.M. Silva, R.J. Silva, M.P. dos Santos, E.G.P. da Silva, M. T. Grassi, M.H. Gonzalez, C.D.B. Amaral, Natural deep eutectic solvent-based microwave-assisted extraction in the medicinal herb sample preparation and elemental determination by ICP OES, *J. Food Compos. Anal.* 109 (2022), <https://doi.org/10.1016/j.jfca.2022.104510>.
- [17] B. Bradić, U. Novak, B. Likozar, Crustacean shell bio-refining to chitin by natural deep eutectic solvents, *Green Process. Synth.* 9 (2019) 13–25, <https://doi.org/10.1515/gps-2020-0002>.
- [18] W. Wang, D.-J. Lee, Lignocellulosic biomass pretreatment by deep eutectic solvents on lignin extraction and saccharification enhancement: a review, *Bioresour. Technol.* 339 (2021), <https://doi.org/10.1016/j.biortech.2021.125587>.
- [19] A. Aghaei, M.A. Sobati, Extraction of sulfur compounds from middle distillate fuels using ionic liquids and deep eutectic solvents: a critical review, *Fuel* 310 (2022), <https://doi.org/10.1016/j.fuel.2021.122279>.
- [20] A.D. Olugbemide, A. Oberlinter, U. Novak, B. Likozar, Lignocellulosic corn Stover biomass pre-treatment by deep eutectic solvents (DES) for biomethane production process by bioresource anaerobic digestion, *Sustainability* 13 (2021) 10504, <https://doi.org/10.3390/su131910504>.
- [21] J.L.K. Mamilla, U. Novak, M. Grilc, B. Likozar, Natural deep eutectic solvents (DES) for fractionation of waste lignocellulosic biomass and its cascade conversion to value-added bio-based chemicals, *Biomass Bioenergy* 120 (2019) 417–425, <https://doi.org/10.1016/j.biombioe.2018.12.002>.
- [22] M.H. Zainal-Abidin, M. Hayyan, G.C. Ngho, W.F. Wong, C.Y. Looi, Emerging frontiers of deep eutectic solvents in drug discovery and drug delivery systems, *J. Control. Release* 316 (2019) 168–195, <https://doi.org/10.1016/j.jconrel.2019.09.019>.
- [23] M.S. Rahman, R. Roy, B. Jadhav, M.N. Hossain, M.A. Halim, D.E. Raynie, Formulation, structure, and applications of therapeutic and amino acid-based deep eutectic solvents: an overview, *J. Mol. Liq.* 321 (2021), <https://doi.org/10.1016/j.molliq.2020.114745>.
- [24] J. Wang, C. Teng, L. Yan, Applications of deep eutectic solvents in the extraction, dissolution, and functional materials of chitin: research progress and prospects, *Green Chem.* 24 (2022) 552–564, <https://doi.org/10.1039/D1GC04340D>.
- [25] K. Chandran, C.F. Kait, C.D. Wilfred, H.F.M. Zaid, A review on deep eutectic solvents: physicochemical properties and its application as an absorbent for sulfur dioxide, *J. Mol. Liq.* 338 (2021), <https://doi.org/10.1016/j.molliq.2021.117021>.
- [26] A. Bjelić, B. Hočevar, M. Grilc, U. Novak, B. Likozar, A review of sustainable lignocellulose biorefining applying (natural) deep eutectic solvents (DESs) for separations, catalysis and enzymatic biotransformation processes, *Rev. Chem. Eng.* 38 (2020) 243–272., <https://doi.org/10.1515/revce-2019-0077>.
- [27] Z. Xue, W. Zhao, T. Mu, Electrochemistry, in: *Deep Eutectic Solvents*, Wiley, 2019, pp. 335–362, doi: 10.1002/9783527818488.ch17.
- [28] S. Opinion, Scientific Opinion on safety and efficacy of choline chloride as a feed additive for all animal species, *EFSA J.* 9 (2011) 1–15, <https://doi.org/10.2903/j.efsa.2011.2353>.
- [29] K. Radošević, M. Cvjetko Bubalo, V. Gaurina Srček, D. Grgas, T. Landeka Dragičević, I. Radojčić Redovniković, Evaluation of toxicity and

- biodegradability of choline chloride based deep eutectic solvents, *Ecotoxicol. Environ. Saf.* 112 (2015) 46–53, doi: 10.1016/j.ecoenv.2014.09.034.
- [30] D.O. Abranches, L.P. Silva, M.A.R. Martins, S.P. Pinho, J.A.P. Coutinho, Understanding the formation of deep eutectic solvents: betaine as a universal hydrogen bond acceptor, *ChemSusChem* 13 (2020) 4916–4921, <https://doi.org/10.1002/cssc.202001331>.
- [31] G. Colombo Dugoni, A. Mezzetta, L. Guazzelli, C. Chiappe, M. Ferro, A. Mele, Purification of Kraft cellulose under mild conditions using choline acetate based deep eutectic solvents, *Green Chem.* (2020) 8680–8691, <https://doi.org/10.1039/d0gc03375h>.
- [32] C. Liu, X. Lu, Z. Yu, J. Xiong, H. Bai, R. Zhang, Production of levulinic acid from cellulose and cellulosic biomass in different catalytic systems, *Catalysts* 10 (2020) 1006, <https://doi.org/10.3390/catal10091006>.
- [33] X. Cheng, Y. Liu, K. Wang, H. Yu, S. Yu, S. Liu, High-efficient conversion of cellulose to levulinic acid catalyzed via functional Brønsted-Lewis acidic ionic liquids, *Catalysis Letters* 152 (2022) 1064–1075, <https://doi.org/10.1007/s10562-021-03701-w>.
- [34] A. Yadav, J.R. Kar, M. Verma, S. Naqvi, S. Pandey, Densities of aqueous mixtures of (choline chloride+ethylene glycol) and (choline chloride+maleonic acid) deep eutectic solvents in temperature range 283.15–363.15K, *Thermochim. Acta* 600 (2015) 95–101, <https://doi.org/10.1016/j.tca.2014.11.028>.
- [35] M.K. AlOmar, M. Hayyan, M.A. Alsaadi, S. Akib, A. Hayyan, M.A. Hashim, Glycerol-based deep eutectic solvents: physical properties, *J. Mol. Liq.* 215 (2016) 98–103, <https://doi.org/10.1016/j.molliq.2015.11.032>.
- [36] A.R. Harifi-Mood, R. Buchner, Density, viscosity, and conductivity of choline chloride + ethylene glycol as a deep eutectic solvent and its binary mixtures with dimethyl sulfoxide, *J. Mol. Liq.* 225 (2017) 689–695, <https://doi.org/10.1016/j.molliq.2016.10.115>.
- [37] M. Rogošić, K.Z. Kučan, Deep eutectic solvents based on choline chloride and ethylene glycol as media for extractive denitrification/desulfurization/dearomatization of motor fuels, *J. Ind. Eng. Chem.* 72 (2019) 87–99, <https://doi.org/10.1016/j.jiec.2018.12.006>.
- [38] A. Yadav, S. Trivedi, R. Rai, S. Pandey, Densities and dynamic viscosities of (choline chloride+glycerol) deep eutectic solvent and its aqueous mixtures in the temperature range (283.15–363.15)K, *Fluid Phase Equilib.* 367 (2014) 135–142, <https://doi.org/10.1016/j.fluid.2014.01.028>.
- [39] H. Moradi, N. Farzi, Experimental and computational assessment of the physicochemical properties of choline chloride/ethylene glycol deep eutectic solvent in 1: 2 and 1: 3 mole fractions and 298.15–398.15 K, *J. Mol. Liq.* 339 (2021), <https://doi.org/10.1016/j.molliq.2021.116669>.
- [40] F. Chemat, H.J. You, K. Muthukumar, T. Murugesan, Effect of l-arginine on the physical properties of choline chloride and glycerol based deep eutectic solvents, *J. Mol. Liq.* 212 (2015) 605–611, <https://doi.org/10.1016/j.molliq.2015.10.016>.
- [41] K.Z. Kučan, M. Perković, K. Cmrk, D. Načinović, M. Rogošić, Betaine + (glycerol or ethylene glycol or propylene glycol) deep eutectic solvents for extractive purification of gasoline, *ChemistrySelect* 3 (2018) 12582–12590, <https://doi.org/10.1002/slct.201803251>.
- [42] F.A. Hatab, A.S. Darwish, T. Lemaoui, S.E.E. Warrag, Y. Benguerba, M.C. Kroon, I. M. AlNashef, Extraction of thiophene, pyridine, and toluene from n-decane as a diesel model using betaine-based natural deep eutectic solvents, *J. Chem. Eng. Data* 65 (2020) 5443–5457, <https://doi.org/10.1021/acs.jced.0c00579>.
- [43] K. Mulia, E. Krisanti, E.L. Nasruddin, Betaine-based deep eutectic solvents with diol, acid and amine hydrogen bond donors for carbon dioxide absorption, *J. Phys. Conf. Ser.* 1295 (2019), <https://doi.org/10.1088/1742-6596/1295/1/012039>.
- [44] A.M. de Castro, D. Prasavath, J.V. Bevilacqua, C.A.M. Portugal, L.A. Neves, J.G. Crespo, Role of water on deep eutectic solvents (DES) properties and gas transport performance in biocatalytic supported DES membranes, *Sep. Purif. Technol.* 255 (2021), <https://doi.org/10.1016/j.seppur.2020.117763>.
- [45] C.Y. Lim, M.F. Majid, S. Rajasuriyan, H.F. Mohd Zaid, K. Jumbri, F.K. Chong, Desulfurization performance of choline chloride-based deep eutectic solvents in the presence of graphene oxide, *Environments* 7 (2020) 97, <https://doi.org/10.3390/environments7110097>.
- [46] M.J. Assael, *The Importance of Thermophysical Properties in Optimum Design and Energy Saving*, in: Energy Environ., Springer Japan, Tokyo, 2001, pp. 162–178, doi: 10.1007/978-4-431-68325-4_7.
- [47] A. Mero, L. Guglielmero, F. D'Andrea, C.S. Pomelli, L. Guazzelli, S. Koutsoumpos, G. Tsonos, I. Stavrakas, K. Moutzouris, A. Mezzetta, Influence of the cation partner on levulinate ionic liquids properties, *J. Mol. Liq.* 354 (2022), <https://doi.org/10.1016/j.molliq.2022.118850>.
- [48] K. Moutzouris, M. Papamichael, S.C. Betsis, I. Stavrakas, G. Hloupis, D. Triantis, Refractive, dispersive and thermo-optic properties of twelve organic solvents in the visible and near-infrared, *Appl. Phys. B* 116 (2013) 617–622, <https://doi.org/10.1007/s00340-013-5744-3>.
- [49] C. Chiappe, P. Margari, A. Mezzetta, C.S. Pomelli, S. Koutsoumpos, M. Papamichael, P. Giannios, K. Moutzouris, Temperature effects on the viscosity and the wavelength-dependent refractive index of imidazolium-based ionic liquids with a phosphorus-containing anion, *PCCP* 19 (2017) 8201–8209, <https://doi.org/10.1039/C6CP08910K>.
- [50] A.P. Abbott, R.C. Harris, K.S. Ryder, Application of hole theory to define ionic liquids by their transport properties, *J. Phys. Chem. B* 111 (2007) 4910–4913, <https://doi.org/10.1021/jp0671998>.
- [51] B.-Y. Zhao, P. Xu, F.-X. Yang, H. Wu, M.-H. Zong, W.-Y. Lou, Biocompatible deep eutectic solvents based on choline chloride: characterization and application to the extraction of rutin from *Sophora japonica*, *ACS Sustain. Chem. Eng.* 3 (2015) 2746–2755, <https://doi.org/10.1021/acssuschemeng.5b00619>.
- [52] Y. Zhang, D. Poe, L. Heroux, H. Squire, B.W. Doherty, Z. Long, M. Dadmun, B. Gurkan, M.E. Tuckerman, E.J. Maginn, Liquid structure and transport properties of the deep eutectic solvent ethaline, *J. Phys. Chem. B* 124 (2020) 5251–5264, <https://doi.org/10.1021/acs.jpcc.0c04058>.
- [53] K. Shahbaz, F.S.G. Bagh, F.S. Mjalli, I.M. AlNashef, M.A. Hashim, Prediction of refractive index and density of deep eutectic solvents using atomic contributions, *Fluid Phase Equilib.* 354 (2013) 304–311, <https://doi.org/10.1016/j.fluid.2013.06.050>.
- [54] K. Shahbaz, S. Baroutian, F.S. Mjalli, M.A. Hashim, I.M. AlNashef, Densities of ammonium and phosphonium based deep eutectic solvents: prediction using artificial intelligence and group contribution techniques, *Thermochim. Acta* 527 (2012) 59–66, <https://doi.org/10.1016/j.tca.2011.10.010>.
- [55] D. Lapeña, L. Lomba, M. Artal, C. Lafuente, B. Giner, The NADES glyceline as a potential Green Solvent: a comprehensive study of its thermophysical properties and effect of water inclusion, *J. Chem. Thermodyn.* 128 (2019) 164–172, <https://doi.org/10.1016/j.jct.2018.07.031>.
- [56] R.B. Leron, A.N. Soriano, M.-H. Li, Densities and refractive indices of the deep eutectic solvents (choline chloride + ethylene glycol or glycerol) and their aqueous mixtures at the temperature ranging from 298.15 to 333.15 K, *J. Taiwan Inst. Chem. Eng.* 43 (2012) 551–557, <https://doi.org/10.1016/j.jtice.2012.01.007>.
- [57] C. Florindo, F.S. Oliveira, L.P.N. Rebelo, A.M. Fernandes, I.M. Marrucho, Insights into the synthesis and properties of deep eutectic solvents based on cholinium chloride and carboxylic acids, *ACS Sustain. Chem. Eng.* 2 (2014) 2416–2425, <https://doi.org/10.1021/sc500439w>.
- [58] M. Lu, G. Han, Y. Jiang, X. Zhang, D. Deng, N. Ai, Solubilities of carbon dioxide in the eutectic mixture of levulinic acid (or furfuryl alcohol) and choline chloride, *J. Chem. Thermodyn.* 88 (2015) 72–77, <https://doi.org/10.1016/j.jct.2015.04.021>.
- [59] O.G. Sas, R. Fidalgo, I. Domínguez, E.A. Macedo, B. González, Physical properties of the pure deep eutectic solvent, [ChCl]:[Lev] (1:2) DES, and its binary mixtures with alcohols, *J. Chem. Eng. Data* 61 (2016) 4191–4202, <https://doi.org/10.1021/acs.jced.6b00563>.
- [60] P.B. Sánchez, B. González, J. Salgado, J. José Parajó, Á. Domínguez, Physical properties of seven deep eutectic solvents based on l-proline or betaine, *J. Chem. Thermodyn.* 131 (2019) 517–523, <https://doi.org/10.1016/j.jct.2018.12.017>.
- [61] F. Mohd Fuad, M. Mohd Nadzir, The formulation and physicochemical properties of betaine-based natural deep eutectic solvent, *J. Mol. Liq.* 360 (2022), <https://doi.org/10.1016/j.molliq.2022.119392>.
- [62] M. Barzegar-Jalali, P. Jafari, A. Jouyban, Thermodynamic study of the aqueous pseudo-binary mixtures of betaine-based deep eutectic solvents at T = (293.15 to 313.15) K, *Phys. Chem. Liq.* (2022) 1–16, <https://doi.org/10.1080/00319104.2021.2024539>.
- [63] L.A. Rodrigues, M. Cardeira, I.C. Leonardo, F.B. Gaspar, I. Radojčić Redovniković, A.R.C. Duarte, A. Paiva, A.A. Matias, Deep eutectic systems from betaine and polyols – physicochemical and toxicological properties, *J. Mol. Liq.* 335 (2021), <https://doi.org/10.1016/j.molliq.2021.116201>.
- [64] H. Monteiro, A. Paiva, A.R.C. Duarte, N. Galamba, Structure and dynamic properties of a glycerol-betaine deep eutectic solvent: when does a DES become an aqueous solution?, *ACS Sustain. Chem. Eng.* 10 (2022) 3501–3512, <https://doi.org/10.1021/acssuschemeng.1c07461>.
- [65] A. Basaiahgari, S. Panda, R.L. Gardas, Effect of ethylene, diethylene, and triethylene glycols and glycerol on the physicochemical properties and phase behavior of benzyltrimethyl and benzyltributylammonium chloride based deep eutectic solvents at 283.15–343.15 K, *J. Chem. Eng. Data* 63 (2018) 2613–2627, <https://doi.org/10.1021/acs.jced.8b00213>.
- [66] M.H. Shafie, R. Yusof, C.-Y. Gan, Synthesis of citric acid monohydrate-choline chloride based deep eutectic solvents (DES) and characterization of their physicochemical properties, *J. Mol. Liq.* 288 (2019), <https://doi.org/10.1016/j.molliq.2019.111081>.
- [67] S.J. Bryant, A.J. Christofferson, T.L. Greaves, C.F. McConville, G. Bryant, A. Elbourne, Bulk and interfacial nanostructure and properties in deep eutectic solvents: current perspectives and future directions, *J. Colloid Interface Sci.* 608 (2022) 2430–2454, <https://doi.org/10.1016/j.jcis.2021.10.163>.
- [68] K.R. Siongo, R.B. Leron, M.-H. Li, Densities, refractive indices, and viscosities of N, N-diethylethanol ammonium chloride-glycerol or -ethylene glycol deep eutectic solvents and their aqueous solutions, *J. Chem. Thermodyn.* 65 (2013) 65–72, <https://doi.org/10.1016/j.jct.2013.05.041>.
- [69] A. Singh, R. Walvekar, W.Y. Mohammad Khalid, T.C.S.M.G. Wong, Thermophysical properties of glycerol and polyethylene glycol (PEG 600) based DES, *J. Mol. Liq.* 252 (2018) 439–444, <https://doi.org/10.1016/j.molliq.2017.10.030>.
- [70] A.P. Abbott, J.C. Barron, K.S. Ryder, D. Wilson, Eutectic-based ionic liquids with metal-containing anions and cations, *Chem. - A Eur. J.* 13 (2007) 6495–6501, <https://doi.org/10.1002/chem.200601738>.
- [71] M. Musiał, K. Malarz, A. Mrozek-Wilczkiewicz, R. Musiol, E. Zorębski, M. Dzida, Pyrrolidinium-based ionic liquids as sustainable media in heat-transfer processes, *ACS Sustain. Chem. Eng.* 5 (2017) 11024–11033, <https://doi.org/10.1021/acssuschemeng.7b02918>.
- [72] C. Florindo, M.M. Oliveira, L.C. Branco, I.M. Marrucho, Carbohydrates-based deep eutectic solvents: thermophysical properties and rice straw dissolution, *J. Mol. Liq.* 247 (2017) 441–447, <https://doi.org/10.1016/j.molliq.2017.09.026>.

- [73] A.Y.M. Al-Murshedi, H.F. Alesary, R. Al-Hadrawi, Thermophysical properties in deep eutectic solvents with/without water, *J. Phys. Conf. Ser.* 1294 (2019), <https://doi.org/10.1088/1742-6596/1294/5/052041>.
- [74] R. Stefanovic, M. Ludwig, G.B. Webber, R. Atkin, A.J. Page, Nanostructure, hydrogen bonding and rheology in choline chloride deep eutectic solvents as a function of the hydrogen bond donor, *PCCP* 19 (2017) 3297–3306, <https://doi.org/10.1039/c6cp07932f>.
- [75] D. Troter, Z. Todorovic, D. Djokic-Stojanovic, B. Djordjevic, V. Todorovic, S. Konstantinovic, V. Veljkovic, The physicochemical and thermodynamic properties of the choline chloride-based deep eutectic solvents, *J. Serbian Chem. Soc.* 82 (2017) 1039–1052, <https://doi.org/10.2298/JSC170225065T>.
- [76] Y. Wang, C. Ma, C. Liu, X. Lu, X. Feng, X. Ji, Thermodynamic study of choline chloride-based deep eutectic solvents with water and methanol, *J. Chem. Eng. Data* 65 (2020) 2446–2457, <https://doi.org/10.1021/acs.jced.9b01113>.
- [77] V. Agieienko, R. Buchner, A comprehensive study of density, viscosity, and electrical conductivity of (choline chloride + glycerol) deep eutectic solvent and its mixtures with dimethyl sulfoxide, *J. Chem. Eng. Data* 66 (2021) 780–792, <https://doi.org/10.1021/acs.jced.0c00869>.
- [78] N.F. Gajardo-Parra, V.P. Cotroneo-Figueroa, P. Aravena, V. Vesovic, R.I. Canales, Viscosity of choline chloride-based deep eutectic solvents: experiments and modeling, *J. Chem. Eng. Data* 65 (2020) 5581–5592, <https://doi.org/10.1021/acs.jced.0c00715>.
- [79] G.L. Burrell, N.F. Dunlop, F. Separovic, Non-Newtonian viscous shear thinning in ionic liquids, *Soft Matter* 6 (2010) 2080, <https://doi.org/10.1039/b916049n>.
- [80] G. Zarca, M. Fernández, A. Santamaría, I. Ortiz, A. Urtiaga, Non-Newtonian shear-thinning viscosity of carbon monoxide-selective ionic liquid 1-hexyl-3-methylimidazolium chloride doped with CuCl, *Sep. Purif. Technol.* 155 (2015) 96–100, <https://doi.org/10.1016/j.seppur.2015.07.032>.
- [81] Y.A. Elhamarnah, M. Nasser, H. Qjblawey, A. Benamor, M. Atilhan, S. Aparicio, A comprehensive review on the rheological behavior of imidazolium based ionic liquids and natural deep eutectic solvents, *J. Mol. Liq.* 277 (2019) 932–958, <https://doi.org/10.1016/j.molliq.2019.01.002>.
- [82] R.K. Ibrahim, M. Hayyan, M.A. AlSaadi, S. Ibrahim, A. Hayyan, M.A. Hashim, Physical properties of ethylene glycol-based deep eutectic solvents, *J. Mol. Liq.* 276 (2019) 794–800, <https://doi.org/10.1016/j.molliq.2018.12.032>.
- [83] Y. Cui, C. Li, J. Yin, S. Li, Y. Jia, M. Bao, Design, synthesis and properties of acidic deep eutectic solvents based on choline chloride, *J. Mol. Liq.* 236 (2017) 338–343, <https://doi.org/10.1016/j.molliq.2017.04.052>.
- [84] G. García, S. Aparicio, R. Ullah, M. Atilhan, Deep eutectic solvents: physicochemical properties and gas separation applications, *Energy Fuel* 29 (2015) 2616–2644, <https://doi.org/10.1021/ef5028873>.
- [85] S.A. Wildman, G.M. Crippen, Prediction of physicochemical parameters by atomic contributions, *J. Chem. Inf. Comput. Sci.* 39 (1999) 868–873, <https://doi.org/10.1021/ci9903071>.
- [86] Y. Cao, T. Mu, Comprehensive investigation on the thermal stability of 66 ionic liquids by thermogravimetric analysis, *Ind. Eng. Chem. Res.* 53 (2014) 8651–8664, <https://doi.org/10.1021/ie5009597>.
- [87] J. González-Rivera, C. Pelosi, E. Pulidori, C. Duce, M.R. Tinè, G. Ciancaleoni, L. Bernazzani, Guidelines for a correct evaluation of Deep Eutectic Solvents thermal stability, *Curr. Res. Green Sustain. Chem.* 5 (2022), <https://doi.org/10.1016/j.crgsc.2022.100333>.
- [88] W. Chen, Z. Xue, J. Wang, J. Jiang, X. Zhao, T. Mu, Investigation on the thermal stability of deep eutectic solvents, *Acta Physico-Chimica Sin.* 34 (2018) 904–911, <https://doi.org/10.3866/PKU.WHXB201712281>.
- [89] Q. Abbas, L. Binder, Synthesis and characterization of choline chloride based binary mixtures, *ECS Trans.* 33 (2010) 49–59, <https://doi.org/10.1149/1.3484761>.
- [90] N. Delgado-Mellado, M. Larriba, P. Navarro, V. Rigual, M. Ayuso, J. García, F. Rodríguez, Thermal stability of choline chloride deep eutectic solvents by TGA/FTIR-ATR analysis, *J. Mol. Liq.* 260 (2018) 37–43, <https://doi.org/10.1016/j.molliq.2018.03.076>.
- [91] G.H. Abdullah, M.A. Kadhom, Studying of two choline chloride's deep eutectic solvents in their aqueous mixtures, *Int. J. Eng. Res.* 12 (2016) 73–80. www.ijerd.com.
- [92] J. González-Rivera, E. Husanu, A. Mero, C. Ferrari, C. Duce, M.R. Tinè, F. D'Andrea, C.S. Pomelli, L. Guazzelli, Insights into microwave heating response and thermal decomposition behavior of deep eutectic solvents, *J. Mol. Liq.* 300 (2020), <https://doi.org/10.1016/j.molliq.2019.112357>.
- [93] H.V.D. Nguyen, R. De Vries, S.D. Stoyanov, Natural deep eutectics as a “Green” cellulose cosolvent, *ACS Sustain. Chem. Eng.* 8 (2020) 14166–14178, <https://doi.org/10.1021/acscuschemeng.0c04982>.
- [94] M. Francisco, A. van den Bruinhorst, M.C. Kroon, Low-transition-temperature mixtures (LTTMs): a new generation of designer solvents, *Angew. Chemie Int. Ed.* 52 (2013) 3074–3085, <https://doi.org/10.1002/anie.201207548>.
- [95] L.K. Savi, D. Carpiné, N. Waszczynskij, R.H. Ribani, C.W.I. Haminiuk, Influence of temperature, water content and type of organic acid on the formation, stability and properties of functional natural deep eutectic solvents, *Fluid Phase Equilib.* 488 (2019) 40–47, <https://doi.org/10.1016/j.fluid.2019.01.025>.
- [96] A. Jani, T. Sohler, D. Morineau, Phase behavior of aqueous solutions of ethaline deep eutectic solvent, *J. Mol. Liq.* 304 (2020), <https://doi.org/10.1016/j.molliq.2020.112701>.